Durham University

Durham E-Theses

Autonomous Droplet Motion on a Surfactant Monolayer

EMRE BABUROGLU

How to cite:

BABUROGLU, EMRE (2020) Autonomous Droplet Motion on a Surfactant Monolayer. Masters thesis, Durham University.

Use policy

The full-text may be used and/or reproduced, and given to third parties in any format or medium, without prior permission or charge, for personal research or study, educational, or not-for-profit purposes provided that:

- a full bibliographic reference is made to the original source
- a https://etheses.durham.ac.uk/id/eprint/13623/ is made to the metadata record in Durham E-Theses
- the full-text is not changed in any way

The full-text must not be sold in any format or medium without the formal permission of the copyright holders.

Please consult the full Durham E-Theses policy for further details.

Academic Support Office, The Palatine Centre, Durham University, Stockton Road, Durham, DH1 3LE
e-mail: e-theses.admin@durham.ac.uk Tel: +44 0191 334 6107
https://etheses.durham.ac.uk

Autonomous Droplet Self-Assembly on a Surfactant Monolayer

Emre Baburoglu

A thesis presented for the degree of
Master of Research

Bain and Kitching Groups
Department of Chemistry
Durham University

December 2019

Autonomous Droplet Self-Assembly on a Surfactant Monolayer

Emre Baburoglu

Submitted for the degree of Master of Research
December 2019

Abstract

Self-propelling droplets have been of much interest as vessels for transporting chemicals without using any external energy and replicating the behaviours of living cells in a synthetic environment. In this study, the underlying mechanism for the spontaneous self-assembly of droplets (4.98 $\pm$ 0.16 μl) of water-immiscible solvents on an aqueous substrate covered in a monolayer of the ionic liquid surfactant trihexyltetradecylphosphonium chloride, $[P_{6,6,6,14}]Cl$, is investigated. The most probable explanation for the mechanism was determined to be the formation of Marangoni flows in the direction of the self-assembling droplets formed by the depletion of the surfactant concentration of the substrate surface surrounding the droplets. This depletion is theorised to occur by the dissolution of the surfactant in the self-assembling droplets when the surfactant molecules are transferred into it along a chemical potential gradient. The amount of the surfactant in a self-assembling droplet (pure benzoyl chloride) and a droplet that does not show self-assembling behaviour (pure mesitylene) were compared after being on the surface of an aqueous substrate covered in said surfactant for 10 minutes was determined using ^{1}H Nuclear Magnetic Resonance (NMR). The amount of surfactant found inside the droplets were 17.5 $\pm$ 2.9 μg and 0 μg respectively. Factors affecting the rate of motion of self-assembling droplets were investigated. The rates of motion of the self-assembling droplets were found to be related to the size of the three phase contact angle. The reason for this was hypothesised to be the change in the speed of the convective flows inside the droplet with changing contact angle. Other observed but unexplained phenomena in this study were presented and possible explanations given.

Declaration

I declare that;

This submission is entirely my own work, and is based in research carried out within the Bain and Kitching Groups at Durham University. No part of this thesis has been submitted elsewhere for any other degree or qualification and each contribution to and quotation in this submission, which is taken from the work or works of other people, has been cited correctly.

Signed: _____

Emre Baburoglu

Copyright © 2019 by Emre Baburoglu.

The copyright of this thesis rests with the author. No quotations from it should be published without the author's prior written consent and information derived from it should be acknowledged.

Acknowledgements

Firstly, I would like to thank Prof. Colin Bain for giving me the opportunity to earn a Master's. This has been an extremely enlightening experience and his expertise has guided me through it. I also thank Dr. Matthew Kitching for his mentorship and going above and beyond the responsibilities of a normal supervisor throughout the year. This experience would not have been what it was without him. Many thanks also to Katherine Carter for developing the code that helped quantify the observations made in this project and the entirety of the Kitching and Bain groups for their companionship, advice and always being willing to help.

Contents

Chapter 1

Background and Literature Review

1.1 The Marangoni Effect

The Marangoni effect is one of those rare phenomena that can be demonstrated easily to impress and attract the attention of both the uninformed and the expert. Marangoni flows are caused by changes in surface tension. Surface tension is the tendency of a liquid to organise itself into its lowest surface area conformation. This is due to the fact that the liquid is more attracted to itself (cohesion) than the air surrounding it. If the surface tension on the surface of a liquid is higher on one part than another, this means that part with higher surface tension possesses a higher attractive force than the other. Hence, liquid flows from the area of low surface tension towards the area of high surface tension due to the molecules of the liquid being more attracted to the area of high surface tension. This is called the Marangoni effect.[1]

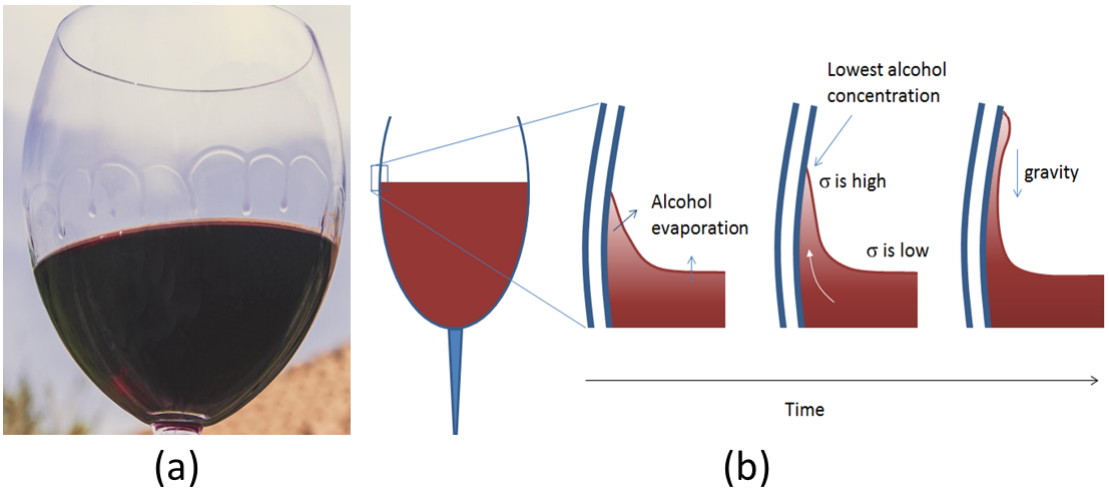

Figure 1.1: (a) The "Tears of Wine" Phenomenon. (b) Liquid rises up the glass due to capillary forces and the difference in surface tension between the sides and the middle of the glass. It then falls down the side of the glass in the form of droplets when gravitational forces dominate. σ denotes surface tension.

1.1. The Marangoni Effect

Figure 1.1(a) shows a glass of wine undergoing the infamous “tears of wine” phenomenon. When wine is poured into a wine glass, tear-like shapes appear running down the side of the glass. This is a classic example of the Marangoni effect. As illustrated in Figure 1.1(b), wine forms a meniscus in the glass due to the adhesive forces between the liquid and the glass being stronger than the cohesive forces within the liquid. Since alcohol is more volatile than water at room temperature, and the liquid on the sides of the glass are thinner than the bulk, regions of low alcohol concentration are created on the sides of the glass. Ethanol has a much lower surface tension than water at room temperature (72.80 mN/m vs 21.80 mN/m) so these regions are also regions of high surface tension. A surface tension gradient is then created and so the liquid flows up the glass via Marangoni flows and capillary action. This continues until the gravitational forces equal the combined force created by the difference in surface tension and capillary action which causes the liquid to flow down the glass creating tear-like shapes on the sides.[2]

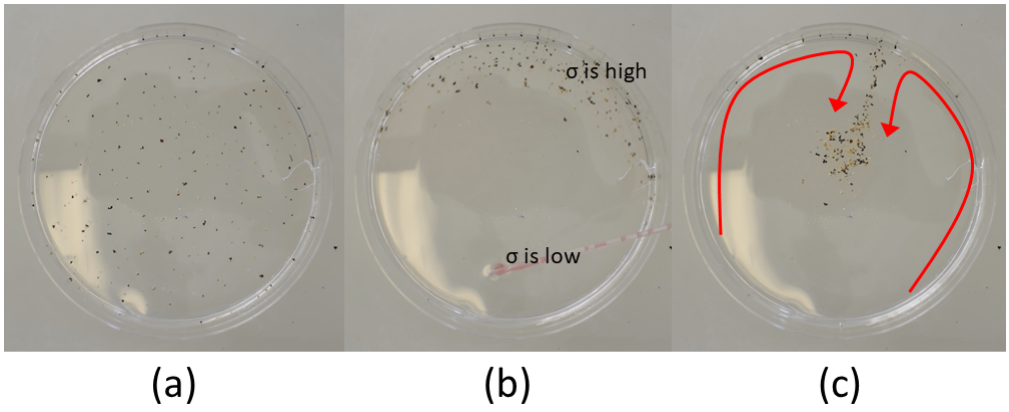

Figure 1.2: (a) Pepper particles initially evenly distributed on the surface of water due to the equal pulling force of the water molecules. (b) When put on the surface, soap lowers the surface tension of water which causes the pepper particles to move away from the source of the soap via Marangoni flows. (c) Pepper particles return towards the centre via convective flows.

Another demonstration of the Marangoni Effect can also be done using a glass of water, pepper (anything that floats on water will do) and any soap. Soap is surface active and has a much lower surface tension than water (or in other words is a surfactant). As shown in figure 1.2(b), when the surface of the water is sprinkled with pepper, if a droplet of soap is dropped on the surface, the pepper moves away from the soap, towards the edges of the dish due to Marangoni flows. One can actually see the shape

of the spreading of the monolayer by the repulsion of the pepper. Once the monolayer of soap is fully spread across the surface of the water, the pepper can move back towards the centre of the dish due to convective flows (Figure 1.2(c)).

1.2 Droplets

1.2.1 Droplet Formation on a Solid Surface

The shape of a droplet is determined by the cohesive forces within the liquid and the external forces that act on it. If there were no external forces, the droplet would be almost perfectly spherical due to a sphere being the shape that has the smallest surface area to volume ratio. The reason a small surface area is favourable is because surface free energy is always positive and minimising the surface area minimises the surface free energy. A reason for the surface free energy being positive is the dispersion interactions between the liquid molecules. In the bulk of the droplet, a given molecule will have more alike molecules around it than one in the surface and hence will have more favourable interactions with the other molecules that lower its free energy than a molecule in the surface. Surface molecules have more interactions with the air, but these are much weaker than the cohesive forces for most liquids and so surface molecules are higher in free energy (Figure 1.3).[3]

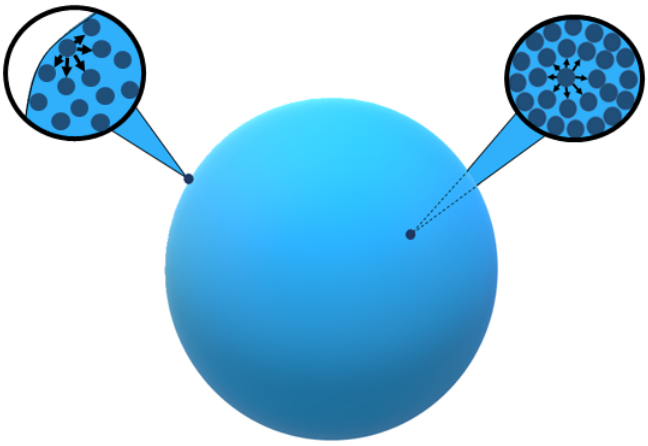

Figure 1.3: A droplet in a theoretical environment where there are no external forces acting on it. Surface molecules have fewer favourable interactions with alike molecules than bulk molecules, therefore the droplet assumes a spherical conformation to minimise surface area.

1.2. Droplets

When on a solid surface, the shape of the droplet is affected by three phases of materials: gas, liquid and solid. The contact angle of the droplet with the solid surface is determined by the balance of the interfacial tensions on the contact line (Figure 1.4). This equilibrium is represented by the Young equation:

$$\gamma_{SV} = \gamma_{SL} + \gamma_{LV}\cos\theta, \tag{1.2.1}$$

where θ is the contact angle the liquid makes with the solid surface and γ_{SV} (solid-vapour), γ_{SL} (solid-liquid), γ_{LV} (liquid-vapour) are the three interfacial tensions. These

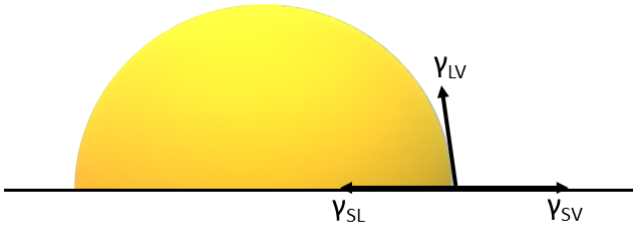

Figure 1.4: A droplet on a solid surface and the interfacial forces acting upon it.

three interfacial tensions determine the initial spreading parameter:

$$S_{\text{liquid-solid}} = \gamma_{SV} - \gamma_{SL} - \gamma_{LV}, \tag{1.2.2}$$

where $S_{\text{liquid-solid}}$ is the initial spreading parameter for a fluid droplet on a solid surface. When $S<0$, the liquid spreads partially. The more negative S is the smaller the area of contact is between the solid and the droplet.[4]

1.2.2 Droplet Formation on a Liquid Surface

When a droplet that is immiscible in the substrate is placed on a surface, there are three outcomes for the morphology: the liquid spreads over the entire surface in order to form a monolayer of uniform thickness (Figure 1.5(a)), the droplet does not spread and stays as a lens (Figure 1.5(b)) or the droplet spreads to form a monolayer but the excess of the droplet is still present as one or more lenses (Figure 1.5(c)).

The morphology is determined by a mixture of long and short-range forces. The effect of short-range forces may be displayed using the equation for the initial spreading coefficient:

$$S_{\text{liquid-liquid}} = \gamma_{LG} - \gamma_{OG} - \gamma_{OL}, \tag{1.2.3}$$

where $S_{\text{liquid-liquid}}$ is the initial spreading coefficient for a fluid droplet on a liquid surface, γ_{OG} (oil-gas), γ_{OL} (oil-liquid), and γ_{LG} (liquid-gas) are the interfacial tensions. If $S>0$, the liquid spreads and when $S<0$ the liquid does not spread.

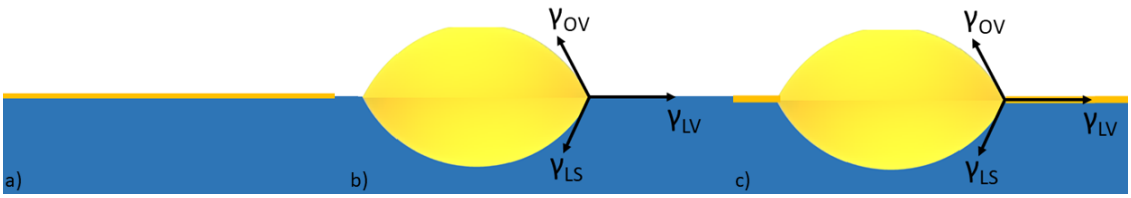

Figure 1.5: a) Droplet spreads over surface forming a film. b) Droplet stays as a lens. c) Droplet spreads to form a film but the excess of the droplet is still present as a lens.

The effect of long-range forces may be understood using the equation for the interfacial free energy of a film of oil:

$$F(D) = \gamma_{OG} + \gamma_{OL} - \frac{A}{12\pi D^2}, \tag{1.2.4}$$

where F(D) is the interfacial free energy of a film of oil of thickness D and A the Hamaker constant that depends on the dielectric properties of the three phases. If $A<0$, the free energy of the film increases as the film gets thicker so spreading is unfavourable. If $A>0$, the free energy of the film decreases as the film gets thicker so spreading is favourable.[5]

1.3 Droplet Self-Assembly

Ordering is a key strategy used to create both life and structure. Whether it is the ordering of living cells to make tissue, or the ordering of bricks to make a house. So, what if we

could get the bricks to order themselves? Self-assembly is the autonomous organisation of particles into patterns or structures without human intervention. It is a behaviour that plays an important role in Nature and in technology. For instance, cells self-assemble into embryonic tissues that further develop into animals. Understanding life will hence involve understanding this behaviour. In nanotechnology, self-assembly is one of the only ways of making ensembles of nanostructures. It will therefore be an essential part of nanotechnology and many more examples come to mind.[6]

One of the reasons droplets are of such interest is because they can be used for compartmentalising and isolating reactants. They are widely used as easily transportable microreactors.[7–11] Due to this characteristic, droplet self-assembly has been used in applications such as high throughput analysis[12], synthesis of nanoparticles[13], fabrication of networks of droplet interface bilayers[14] and self-patterning of materials.[15,16] Although, despite potential applications ranging from reagent mixing to spray coating, there has not been much work done on droplet self-assembly on an air-water interface.[42]The droplet self-assembly system discussed in this thesis addresses this niche.

The system investigated in this study involved two oil droplets (contents discussed later) moving towards each other on an aqueous surface (0.1 M HCl, 0.1 M NaOH, 0.1 M H_2SO_4) covered in a monolayer of the ionic liquid (IL) trihexyltetradecylphosphonium chloride (Figure 1.6) as the surfactant. The objective was to determine the underlying mechanism behind the motion of the self-assembling droplets. In this chapter, reports of possible explanations for the spontaneous motion of droplets are explored.

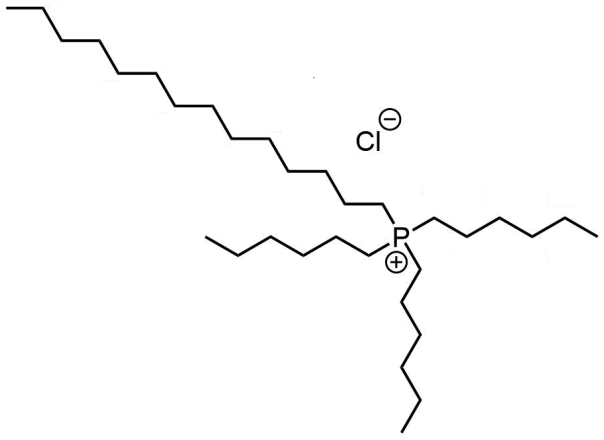

Figure 1.6: Structure of the ionic liquid trihexyltetradecylphosphonium chloride used in this study.

1.4 Droplet Motion on a Liquid Surface

Self-propelling droplets have been of much interest as vessels for transporting chemicals without using any external energy. This is done using Marangoni flows since they convert chemical energy that is already inside the droplet or on the surface of the solvent to kinetic energy for the motion of the droplet. The study of moving droplets is widely associated to motions of living cells. From a purely structural perspective, cells are just spherical droplets trying to minimise their surface energy.[17] The difference is that cells show tactic behaviour in response to external stimuli such as temperature, electric fields and chemical gradients.[18–21] In this review, I will explore the efforts made in literature in order to replicate these living cell behaviours in droplet systems and other mechanisms in which droplet motion might be achieved. These will be separated into two sections: random droplet motion and directional droplet motion. Random droplet motion is motion caused by a spontaneous breakage in the symmetry of the internal or external flows of the droplet. Directional droplet motion happens when this symmetry breakage happens in a manner such that the droplet moves towards a specific location. In order to determine the mechanism of a droplet motion system, one must consider the origin and effect of both types of motion.

1.4.1 Random Droplet Motion

Motion Due to Chemical Reaction

In systems containing surfactant, chemical reactions that cause a change in the surfactant medium can create a Marangoni flow and hence make the droplet move. This has been achieved in many ways.[22–25] A good example was demonstrated by Suematsu *et al.*[26]. When an aqueous droplet of sodium bromate (0.4 M) and sulfuric acid (0.0-1.8 M) is placed in an oil medium (squalane) containing monoolein (0.1 or 10 mM), the aqueous droplet shows spontaneous motion. The bromination of monoolein lowers the surface tension of the surfactant. When the aqueous droplet is placed in the oil medium, it is covered in monoolein (MO) surfactant. Simultaneously, the bromate inside the droplet is protonated by the sulfuric acid and reacts with oxygen to form bromine as shown in the equations below.

$$BrO_3^- + H^+ \longrightarrow HOBr + O_2$$

$$4\,HOBr \longrightarrow 2\,Br_2 + 2\,H_2O + O_2$$

The bromine then reacts with the MO, as shown in Figure 1.7(a), to form brominated MO (MOBr). The random and hence asymmetric bromination of MO causes the formation of surface tension gradients along the oil-aqueous interface. These then generate convective flows inside the droplet that propel it towards the side of the bromination.[26] The reaction shown on Figure 7(a) is suprising considering that one would expect bromine to attack the carbon-carbon double bond.

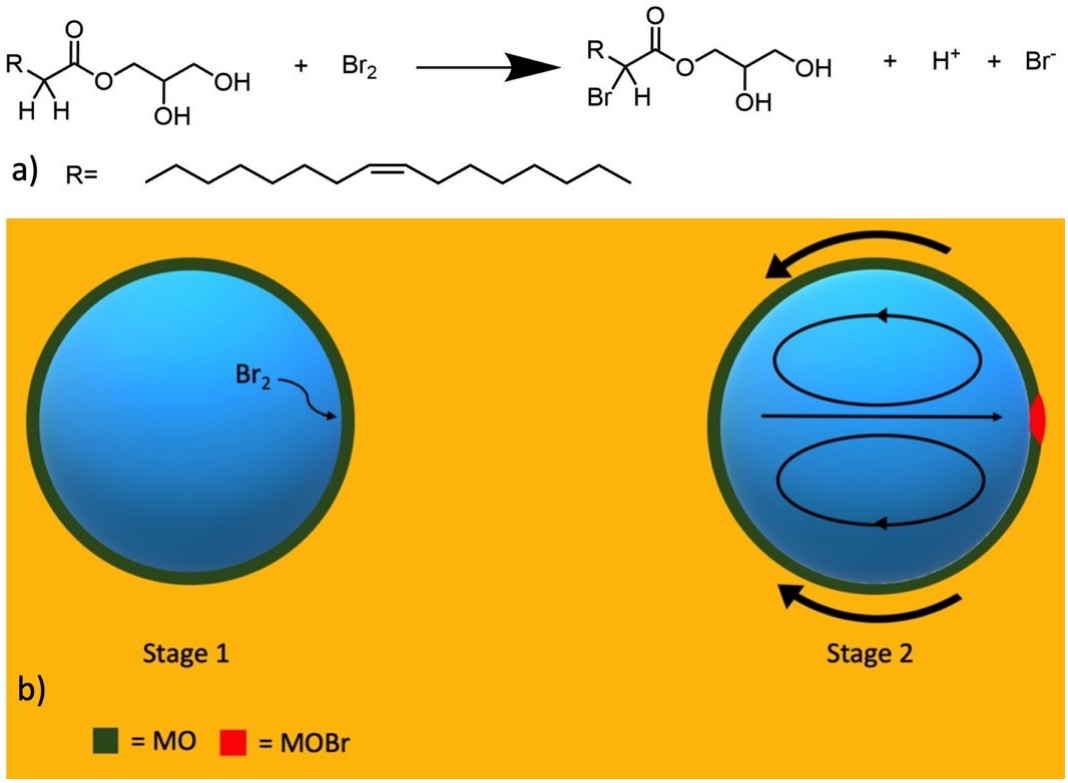

Figure 1.7: a) The bromination of monoolein occuring in the oil-droplet interface.b) Two-dimensional schematic of the mechanism for droplet motion. Stage 1: The aqueous droplet is covered in monoolein surfactant. Stage 2: The bromine inside the droplet asymmetrically reacts with the surfactant coating the droplet to form MOBr, which is a better surfactant than MO. A surface tension gradient is generated along the interface causes the formation of internal convective flows within the droplet that propel it in the direction of the site of bromination. Arrow inside the droplet shows direction of movement.

Convective Flows

Convective flows in the case of droplets is the transfer of mass due to the bulk motion of a fluid. This can be caused by external stimuli such as surface tension or chemical gradients. Although the notion of external convective flows causing droplet motion might seem obvious, according to Matsuno *et al.*[27], convective flows inside the droplet also aid and can sustain its motion (Figure 1.8). Through mathematical simulations they found that although a chemical gradient was necessary, the rate was slower without the convective flow inside the droplet.[27] This effect is present in some form in most of the mechanisms cited in this review.

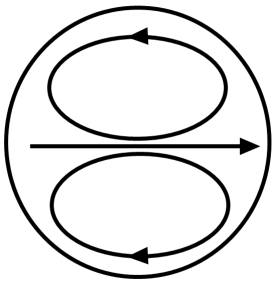

Figure 1.8: Convective flows inside a droplet that aid it's movement. The arrow in the middle is the direction of motion of the droplet.

Maass *et al.*[28] report that convective flows can also cause change in the type of motion of droplets. When convective flows are coupled to the nematic director field, a symmetry breakage occurs which causes the droplet to move in a helical trajectory (Figure 1.9).[28]

Motion Due to Micellar Distribution

Micelles form when the amount of surfactant added to the solution is above the critical micellar concentration (CMC). It is the concentration at which the chemical potential of a surfactant in solution is the same as that in an aggregate (micelle). A micelle is a colloid of aggregated surfactants in the bulk. In order to minimise their free energy, the surfactants arrange with their hydrophilic heads pointing out and hydrophobic tails pointing in. In their Jan 2018 publication, Jin *et al.*[29,30] have claimed that droplets can be propelled via micellar solubilisation. Their system consists of water, a cationic surfactant and an oil droplet that is sparingly soluble in water. When the concentration of surfactant added surpasses the CMC, micelles form and are repelled from the immersed oil droplet due to

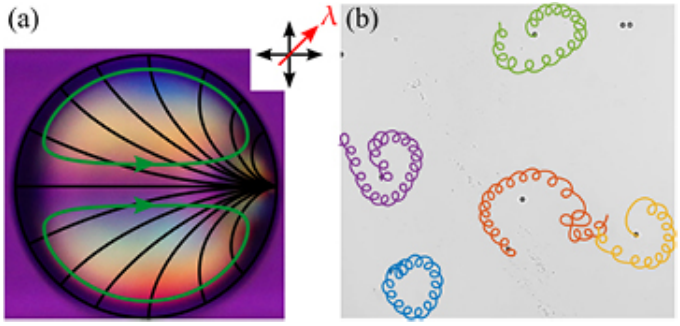

Figure 1.9: (a) A polarised micrograph of a self propelling droplet with superimposed sketches of its nematic director field (black lines) and the convective flows inside it (green lines). (b) Pattern of helical swimming as a result of symmetry breakage caused by the coupling of the convective flows to the nematic director field. Figure taken from Ref 28.

their charge. When some of the oil dissolves into solution, the micelles around it swell in order to accommodate the oil. This then depletes the concentration of free surfactants in the solution to below the CMC which causes the empty micelles to disintegrate to replenish the CMC. Filled micelles are stabilised by the incorporation of the oil. When the droplet is displaced by a random autophoretic motion, the cloud of filled micelles is left behind it and so the interfacial surfactant coverage in its front is increased. Convective flows towards the posterior of the droplet along the interface are hence generated and the droplet propelled forward (Figure 1.10).[29,30]

Another way micelles could cause droplet motion is by adsorbing onto the droplet surface. If we consider a droplet immersed in fluid and not covered in surfactant, when a micelle comes into contact with that droplet, convective flow within the droplet are generated which cause it to be propelled towards the adsorption point, similarly to the previous example. The resulting outer flow of the liquid then advects micelles towards the adsorption site making the droplet move in only that direction (Figure 1.11).[31]

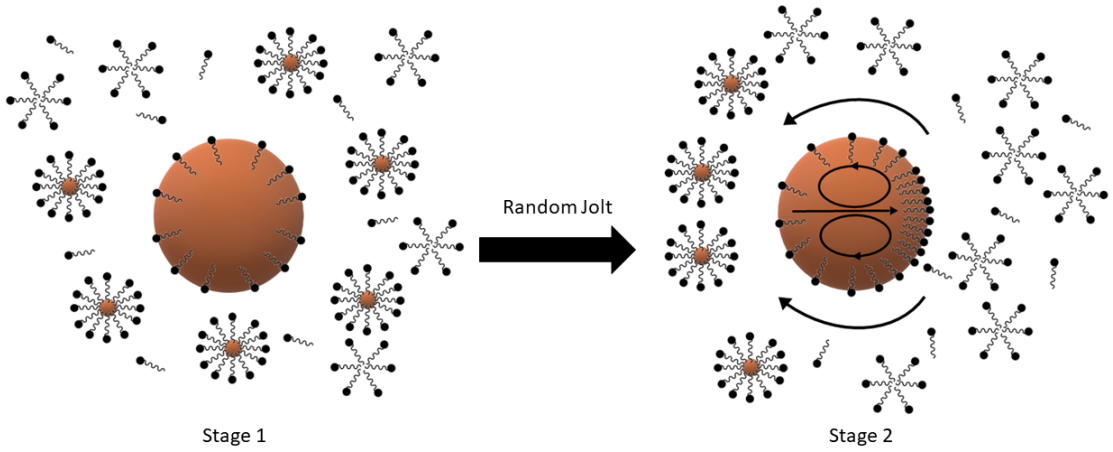

Figure 1.10: Stage 1. Droplet is surrounded by filled micelles and is in equilibrium. Stage 2. A random jolt causes the droplet to move away from the filled micelles. The anterior side of the droplet is then exposed to a higher concentration of unfilled micelles and hence free surfactants. The free surfactants adsorb onto the anterior side of the droplet and create a surface tension gradient and hence Marangoni flow along the interface. This results in convective flows inside the droplet that propel it forward.

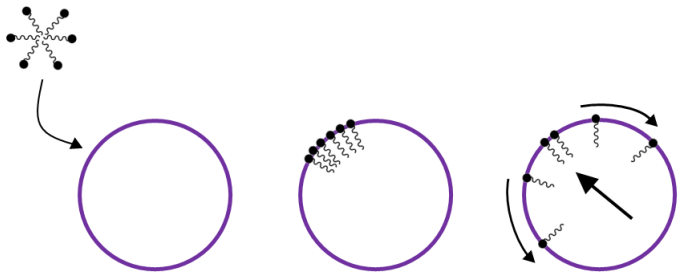

Figure 1.11: A micelle adsorbing on to the droplet causing motion towards the adsorption site.

Chemical Potential Gradients

Chemical potential describes the change in Gibbs free energy when the number of particles in a component of a system changes. Since systems tend to try to minimise the Gibbs free energy of a system, chemical potential determines the direction in which the system can move in order to achieve this. The two equations for chemical potential of concern here are:

$$\mu_i = \left(\frac{\partial G}{\partial n_i}\right)_{p,T,n_j \neq i}, \tag{1.4.5}$$

$$\mu_i = \mu_0 + RT\ln(x_i), \tag{1.4.6}$$

where μ_i is the chemical potential of the ith species in the mixture, μ_0 is the chemical potential of pure species i, R is the gas constant, T is temperature, x_i is the mole fraction of species i contained in the ideal mixture, G is Gibbs free energy, p is pressure and n_i is the number of particles of species i. According to equation (1.4.6), the chemical potential of a species and hence the Gibbs free energy of a system increases when the mole fraction of that species increases. Therefore, in a two-component system, if one location has a higher concentration of a substance than the other, the substance will be transferred from a higher concentration to low because this process is accompanied by a decrease in Gibbs free energy.[32] This is called a chemical potential gradient.

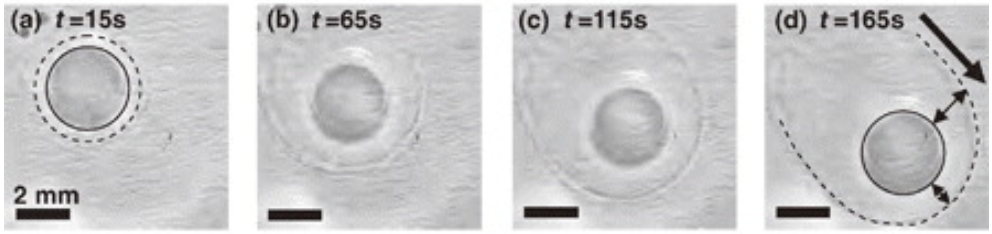

Figure 1.12: (a) The concentration gradient between the droplet and the solution is isotropic so there is no motion. (b)-(d) When the droplet moves slightly, the variation in concentration on it's leading edge becomes narrower which results in a steeper concentration gradient and a stronger Korteweg force in that direction. Figure taken from Ref 33.

In their September 2010 publication, Ban *et al.*[33] have used this basic principle to incite droplet motion. When an aqueous droplet of differing concentration of a substance to the solution is put on an aqueous solution, a concentration gradient is formed. This concentration gradient causes an interfacial energy to arise along the liquid-liquid contact

line creating a composition dependent force called the Korteweg force which generates convective flows that propel the droplet forward. In their study, Ban *et al.*[33] put a droplet containing a higher concentration of polyethyleneglycol and sodium sulphate into a solution of lower concentration of said chemicals. Initially the droplet is motionless as the concentration gradient is present in all sides of the droplet. When the droplet moves slightly, the concentration gradient on its leading edge becomes steeper than the other sides and hence the Korteweg force increases in that direction (Figure 1.12). The concentration gradient in the leading edge of the droplet is replenished as it moves in this way leading to sustained motion.[33]

1.4.2 Directional Motion and Self-Assembly

Diffusiophoresis

Diffusiophoresis is the phenomenon where, when a particle is placed in a fluid in which there is a non-uniform concentration of solute, the particle will move towards the higher or lower concentration of that solute depending on the particle's preference. In non-electrolyte solutions, this happens due to a non-uniform distribution of a chemical in the solution. An example of this is the Marangoni effect where particles move from a high concentration of surfactant to low.[34] In non-uniform electrolyte solutions this occurs when a charged particle moves towards a higher or lower concentration of the electrolyte in the solution depending on its charge. This happens in two ways: first, a macroscopic electrolyte gradient produces an electric field which acts on the charged particle and then the electrolyte gradient polarises the cloud of counterions surrounding the charged sphere by making the cloud thinner on the high concentration side.[35]

A great example of diffusiophoresis is given by Abecassis et al where they inject silica particles into a trident shaped channel and observe the changes in the path of motion of the silica particles depending on the distribution of the salt ions. They alternate the channels to which the salt solution (10 mM LiCl, NaCl or KCl) is added and observe the path of the motion of the silica particles (Figure 1.13).[36]

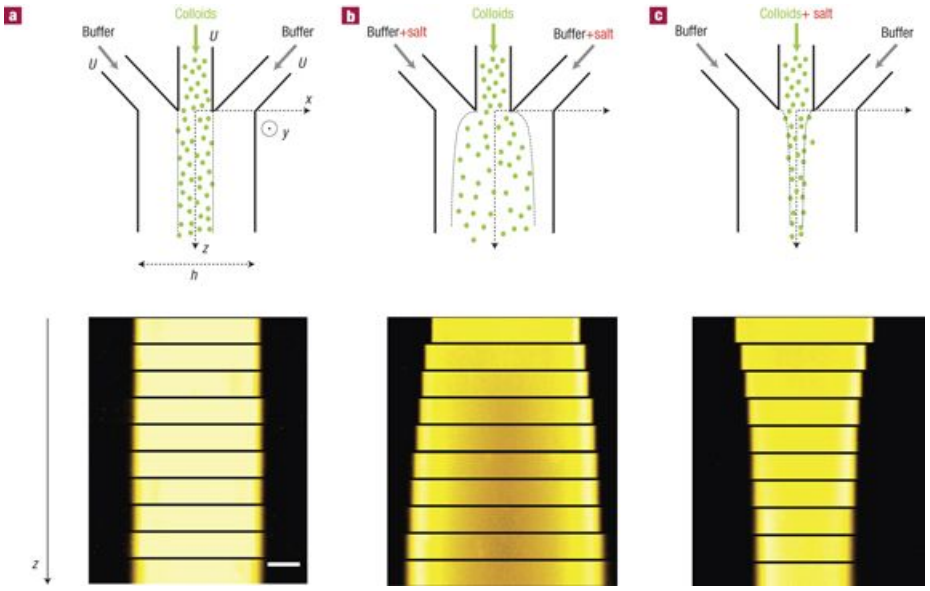

Figure 1.13: (a) Control experiment where there is no salt solution (10 mM LiCl, NaCl or KCl) added. The path of the silica remains stationary. (b) Salt solution added through the side channels. The silica spread to the sides while flowing through the channel when salt concentration gradient imposed. (c) Salt solution added through the same channel as the silica. The silica pursue a narrower path. Figure taken from Ref 36.

Asymmetric Release of Surfactant

If a droplet on the surface of a liquid is programmed to release surfactants in the opposite direction of a chemical stimulus, that droplet will move towards that stimulus. Francis *et al.*[37] have demonstrated this effect using a droplet of the ionic liquid (IL) trihexyltetradecylphosphonium chloride ($[P_{6,6,6,14}]Cl$) as the surfactant and the droplet on water. They claim that by placing a droplet of the IL into a microfluidic channel with a Cl^- gradient biases the release of the cationic surfactant $[P_{6,6,6,14}]^+$ from the droplet away from the source of the chloride gradient (Figure 1.14). This results in the generation of Marangoni flows towards the Cl^- source. This experiment has also been done using KBr and Na_2SO_4 instead of HCl, implying that this behaviour can be affected by any factor altering the ionic equilibria.[37]

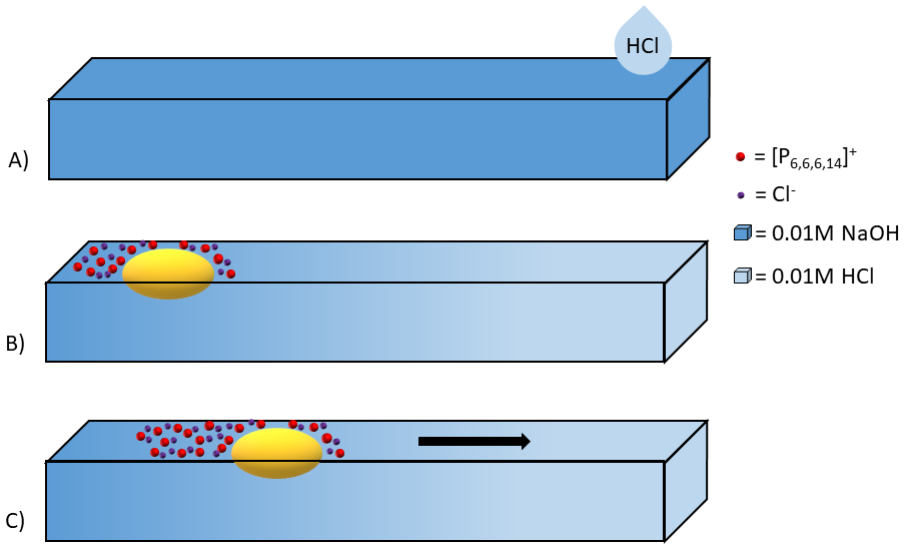

Figure 1.14: A) 0.01M HCl added to one end of the channel establishing a Cl^- gradient. B) The IL droplet is added and it releases more surfactant away from the source of the Cl^- ions due to the solubility of the $[P_{6,6,6,14}]Cl$ complex. C) Droplet starts moving towards the source of the Cl^- ions due to Marangoni flows created by this surface tension gradient.

Vapour-Induced Self-Assembly

Asymmetric droplet evaporation can be used to create surface tension gradients across the droplet resulting in motion. Prakash *et al.*[38] have constructed a system where two droplets consisting of similar proportions of water and propylene glycol (PG) will find each other in a clean solid surface. The mechanism is based on the fact that water has a much higher vapour pressure than PG and so water is the dominant vapour and that PG has a lower surface tension than water. When the droplets are next to each other, there hence is an increase in the external humidity between the droplets and decreased evaporation of the side of the droplet that is nearer the other droplet (Figure 1.15). This causes a breakage in symmetry and an increased proportion of water on the side of the droplet adjacent to the other droplet and hence increased surface tension locally. The difference in surface tension around the droplets makes them move together.[38]

Another way evaporation can be used to generate Marangoni flow is simply by using the latent heat of evaporation of the droplets. Liu *et al.*[16]. found that if two droplets of 50% isopropyl alcohol (IPA) in aqueous solution are deposited on a surface of silicone oil, they will self-assemble. This is due to the high volatility of IPA. Both droplets cool their surroundings via evaporation and the result is that the surface is coldest in between the

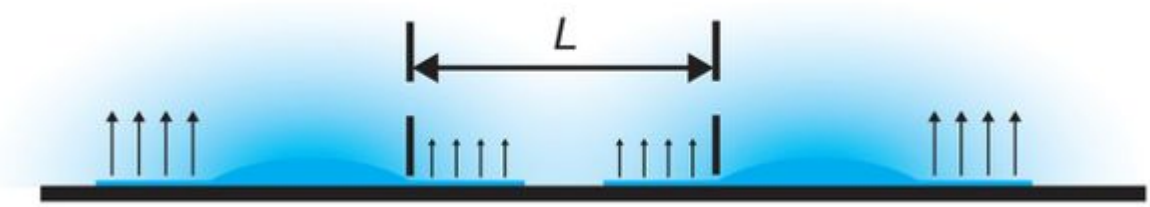

Figure 1.15: Decreased evaporation of water on the shared side of the droplets. More water and hence higher surface tension on the shared side of the droplets propel them together via Marangoni flows. Evaporation shown by the black vertical lines. Figure taken from Ref 38.

two droplets. This raises the surface tension between the droplets relative to elsewhere on the surface and creates a Marangoni flow towards that area (Figure 1.16).[16]

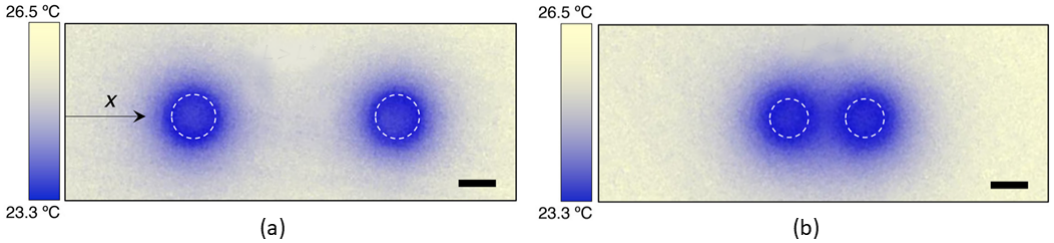

Figure 1.16: (a) Droplets evaporate and hence cool the liquid surface around them. (b) The decrease in temperature of the area between the droplets increases its surface tension which makes the droplets assemble. Figure taken from Ref 16.

Electrostatic Interactions

Electrostatic interactions can also be used to generate directional motion depending on the nature of the surfactant. Ban *et al.*[39], have created a system where a submerged droplet consisting of nitrobenzene and 0.1M di-(2-ethylhexyl)phosphoric acid (DEHPA) can be used to extract metal ions from an aqueous solution. The authors suggested source of motion in this mechanism is deprotonated DEHPA which acts as a surfactant and causes the droplet to exhibit random motion by creating asymmetric surface tension gradients. The motion is made directional when a metal ion from the solution binds to the negatively charged surfactant creating a DEHPA-metal complex and subsequently desorbing from the interface. The desorption causes a change in interfacial energy that creates convective flows that propel the droplet towards areas of higher metal ion con-

centration (Figure 1.16).[39]

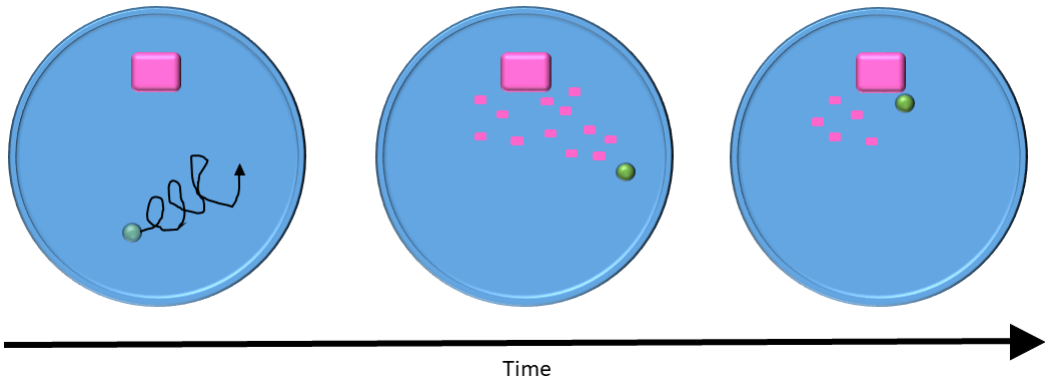

Figure 1.17: Droplet first shows random motion in the petri dish due to the DEHPA being deprotonated in pH 7.41 buffer solution (black arrow). Droplet then moves towards the metal ion source (Mg^{2+},Ca^{2+}, Sr^{2+} or Ba^{2+}), extracting the ions along the way. Metal ion source shown in pink.

Another way of causing droplet motion using electrostatic interactions is by manipulating the distribution of ion in a solution. Diamond *et al.*[40] report doing this using a system composed of a microfluidic channel filled with an aqueous solution of NaCl, two titanium electrodes at either end of the channel and a droplet of IL ($[P_{6,6,6,14}]Cl$). As explained before, a droplet of this IL will move against a chloride ion concentration gradient. The suggested mechanism is that a chloride gradient is generated by applying an external electric field across the solution which made the sodium ions move towards the anode and the chloride ions move towards the cathode. Hence, the IL droplet moves towards the cathode (Figure 1.17).[40]

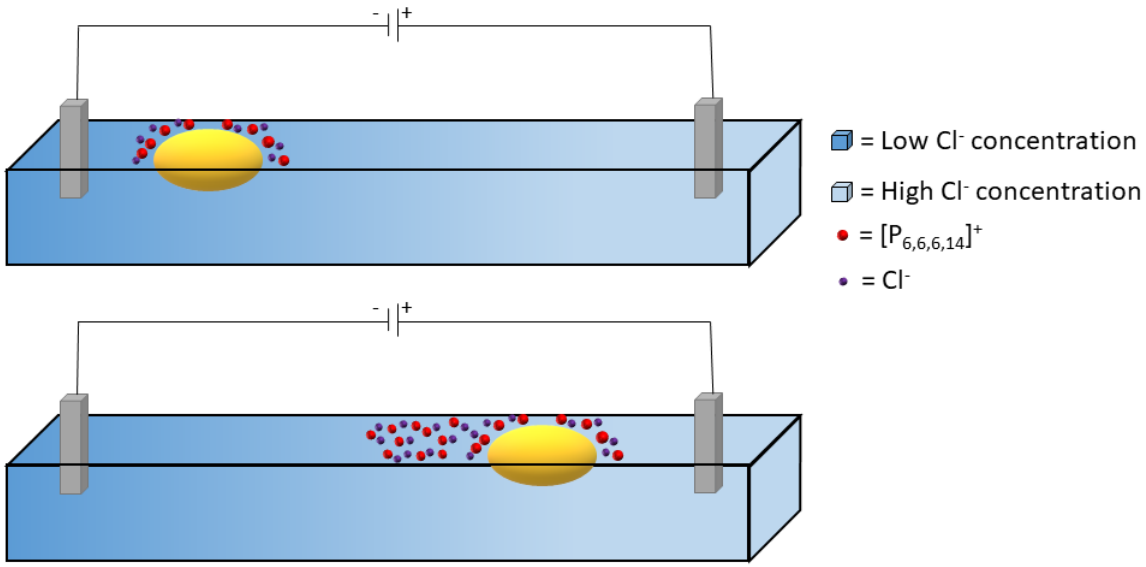

Figure 1.18: The IL droplet moves towards the hgher concentration of Cl^- ions located at the cathode due to the asymmetric solubility of the surfactant.

Directional Motion caused by a difference in pH

By picking the right surfactant, directional droplet motion can also be achieved using a H^+ ion gradient. Lagzi *et al.*[41] managed to make a droplet consisting of 2-hexyldecanoic acid (HDA) and dichloromethane (DCM) navigate the shortest path through a maze using this effect. The experiment was done in a KOH solution of pH 12.0-12.3 with an acidic gel in one end of the maze. The droplet spontaneously moves towards the acidic gel. My interpretation of their conclusion is that this is due to the higher surface activity of deprotonated HDA compared to protonated HDA. The asymmetric increase in the concentration of protonated HDA in the direction of the acid causes a Marangoni flow towards the acid which results in droplet motion.[41] Although, this paper is confusing for a number of reasons. It states that deprotonated HDA is much less surface active than protonated HDA which, in my interpretation, must be a typo for the motion to occur as it is reported since if not, the droplet would move in the opposite direction. However, it would make sense that deprotonated HDA is less surface active than protonated HDA since ions are more soluble than neutral molecules. For this reason, I believe there must be something else going on.

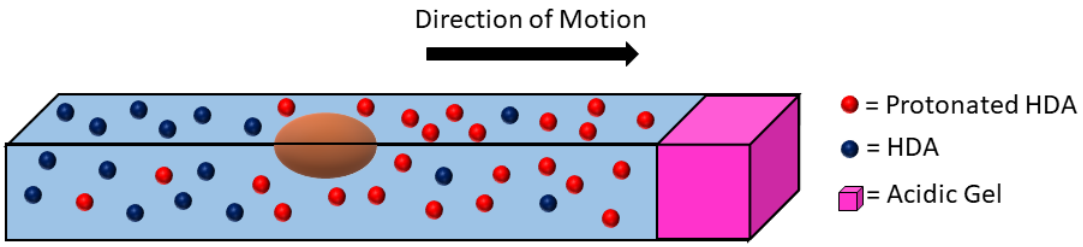

Figure 1.19: Droplet moves towards area of high pH due to the protonation of the surfactant.

Motion Caused by Coalescence

Droplet motion can occur post-coalescence. Sellier *et al.*[42] showed that when two droplets of differing surface tensions coalesce, the Marangoni flows resulting from the surface tension gradient propel the droplets in the direction of the high surface tension droplet (that has now merged). The propulsion continues until the ”fuel”, which is the surface tension gradient, runs out.

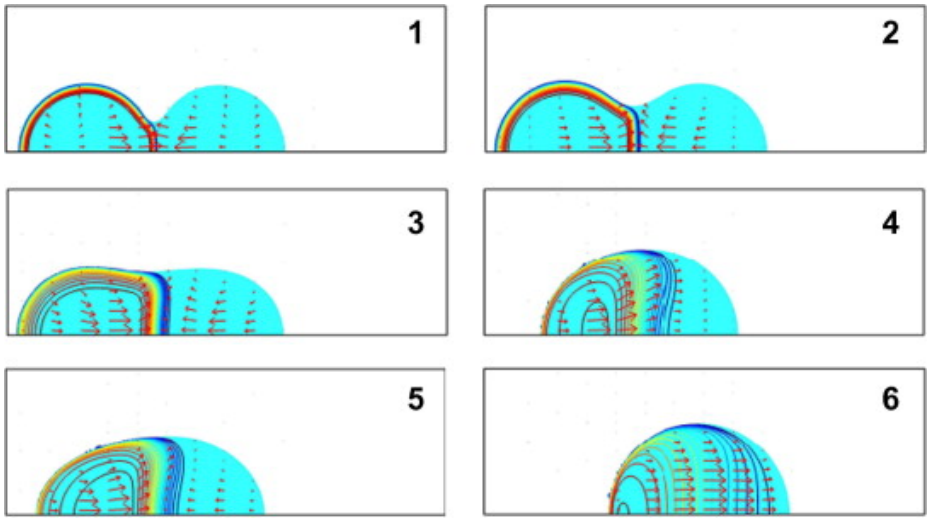

Figure 1.20: Vector plot (red arrows) of the volumetric discharge field and contours of constant surface tension with time increasing from figure 1 to 6. The droplets merge and the resulting droplet is propelled towards the side of the high surface tension droplet via Marangoni flows. Figure taken from Ref 42.

The two variables that govern the rate of this motion are Σ, a measure of the surface tension contrast and d, diffusivity. The propulsion is enhanced by greater Σ due to the increased strength of the Marangoni stresses propelling the droplet and smaller d due to

the prolonging of the surface tension gradient. Greater Σ increases the fuels power, and reduced d increases the amount of fuel.[42]

Cheerios Effect

The Cheerios effect, affectionately named after the observation that floating cereal in a bowl full of milk clump together, is an effect that should be considered by all who are doing research on droplet coalescence on liquid surfaces. The Cheerios effect is a gravitational effect where when two nearby droplets bend the surface of the liquid, they spontaneously aggregate. An easy way to understand this is to picture the surface of water as the skin of a trampoline and the two droplets as heavy balls. Due to the deformation of the trampoline, the two heavy balls will go towards each other. This is not usually a long-range affect with droplets but should always be considered.[43]

Figure 1.21: Metal pin bending the surface of water.

1.4.3 Conclusion

Using droplets is a way of replicating the behaviours of cells inside the body in a synthetic environment. They also have various uses ranging from metal extraction to chemical patterning if their motion can be controlled. As discussed, this can be done in a number of ways and all should be considered when doing research on a specific system. Despite this, most of the mechanisms require a complicated variety of components in very specific conditions. A directional droplet motion system where the motion of an extensive variety of different droplets on a range of aqueous surfaces can be explained by the same, simple mechanism has not yet been reported. In this study, I will discuss the mechanism of such a system.

1.5 Thesis Approach

At the start, the system investigated in this project consisted of two droplets of 4 M benzoyl chloride in IL, on the surface of an aqueous substrate, in a petri dish caused to move towards each other and coalesce by a droplet of 0.5 M octylamine dissolved in IL placed later onto the surface (further details in the Experimental section). The motivation for this research project was to try to understand the mechanism with which this happens. Once the most likely mechanism was determined, different ways of controlling the rate of the process were explored to better understand the features of the system needed to recreate this behaviour in a different setting.

The first approach I took in order to determine the underlying mechanism was to vary the parameters involved in the system such as the contents of the aqueous substrate, concentration of the droplets and the order in which the droplets were placed on the surface to find out what was necessary for the motion to occur. The substrates used were: pH 4 0.1 M acetic acid buffer, pH 7 0.1 M phosphate buffer and pH 10 0.1 M carbonate buffer in order to check if pH change was part of the underlying mechanism, 0.1 M HCl, 0.1 M NaOH, 0.1 M H_2SO_4 and water in order to understand the affects of the change in pH on the system, 0-3 M glucose in order to understand the affect of the increase in the density of the substrate on the motion and saturated NaCl solution in order to rule out the existence of a possible chloride gradient such as the one reported by Francis *et al.*[37] The droplets showed self-assembly in all of the mentioned substrates so they were eliminated as parameters that were important to the origin of the underlying mechanism of motion. By changing the order of the droplets being placed on the aqueous surface, Katherine Carter found that the same self-assembly could be achieved when the 0.5 M octylamine droplet was placed on the surface before the self-assembling droplets. By changing the concentrations of the droplets, I found that the IL inside the 4 M benzoyl chloride droplets and the octylamine in the 0.5 M octylamine droplets were not necessary for the motion to occur. I also found that benzoyl chloride could be swapped for other solvents as the constituent of the self-assembling droplet. I then simplified the system to two oil droplets moving towards each other on a monolayer of IL surfactant.

The next approach was to come up with hypotheses to explain the underlying mechanism and the reasons behind the factors that affected the motion. Experiments were then designed in order to reject them. Most were successfully rejected. The evidence for

and against some of these hypotheses are explained in the Results and Discussion section. Lastly, in order to quantify the observations, we used analytical techniques including: the Wilhelmy plate method, MatLab code developed by Katherine Carter, ^{1}H NMR and HSPiP software. This is discussed further in the Experimental section.

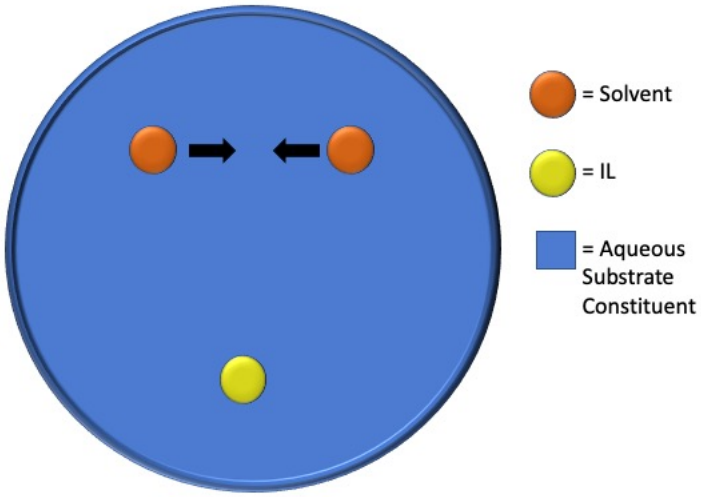

Figure 1.22: A petri dish schematic outlining the standard petri dish experiment. Throughout the project, the aqueous substrate constituents used were differing concentrations of: HCl, NaOH, H_2SO_4, glucose, NaCl, Na_2SO_4. The solvents used were: Benzoyl chloride, methyl benzoate, chloroform, dichloromethane, toluene, hexane, hexadecane and mesitylene. The solvents in the droplets contained varying concentrations of IL when required.

Chapter 2

Experimental

2.1 Experimental Set-up

2.1.1 Petri Dish Procedure

Unpublished results by Dr. Matthew Kitching *et al.* found that two drops of 4 M benzoyl chloride in the ionic liquid trihexyltetradecylphosphonium chloride(IL) on an aqueous surface (0.1 M HCl, 0.1 M NaOH, 0.1 M H_2SO_4) on a petri dish (plastic, 9 cm diameter) find each other and coalesce on the surface if they are activated by a drop of 0.5 M octylamine in IL dropped on the surface. We later discovered that the octylamine in the activating droplet and the IL in the benzoyl chloride droplets were not necessary for this effect to occur and solvents other than benzoyl chloride could be used as self-assembling droplets. The experimental procedure was thus changed to dispensing a drop of IL (25.8 $\pm$ 0.3 μl) using an Injekt®- F Solo 1 ml syringe with no needle and two (or more) drops (4.98 $\pm$ 0.16 μl) of the oil (self-assembling droplet) with an Injekt®- F Solo 1 ml syringe with a Microlance®3 metal needle (1.1 mm diameter, 40 mm length). A typical experimental petri-dish procedure is shown in Figure 2.1(b). It consists of an array of 8-by-4 array of green LED lights lodged onto the side of a polystyrene box, with a frosted glass plate over the top of the box, under where the petri dish would be and a camera (Nikon D5300, 50 fps, 50-mm lens) to film the motion (Figure 2.1(a)). The lighting is used to get rid of any shadows that might interfere with image processing by Matlab code.

2.1.2 Suspended Droplet Procedure

The suspended droplet procedure refers to an effect that was discovered when investigating the effect mentioned above. When a drop of IL is dropped onto an aqueous solution of 0.1 M HCl and a droplet of a solvent is suspended over the surface, objects floating on the surface assemble under this droplet. The floating objects in this case are flakes of pepper. The set-up is shown in Figure 2.2.

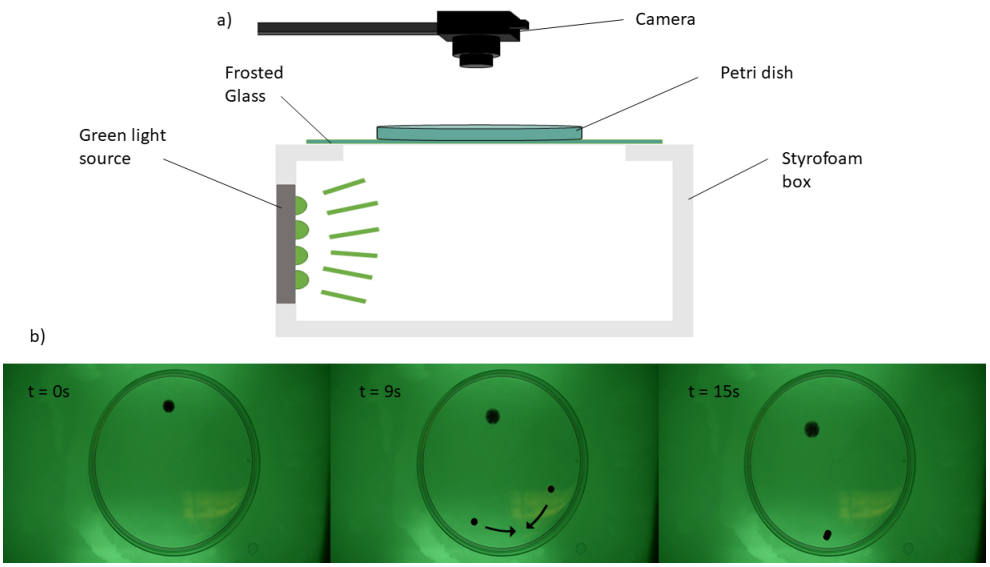

Figure 2.1: a) A side-on schematic of the experimental set-up where the petri dish is set on top of frosted glass which is set over the top of a hollow styrofoam box. An 8-by-4 green LED light source is place in the side of the box. The camera is placed directly above for filming. b) Time lapse of a typical experiment. All droplets are dyed using Rhodamine B for better visualisation for this figure. Dyes are not used in normal experimental conditions. t = 0 s: A drop of IL is put on the surface of a solution of 0.1 M HCL. t = 9 s: Two drops of benzoyl chloride are put on the surface and start moving towards one another. t = 15 s: The two benzoyl chloride droplets coalesce.

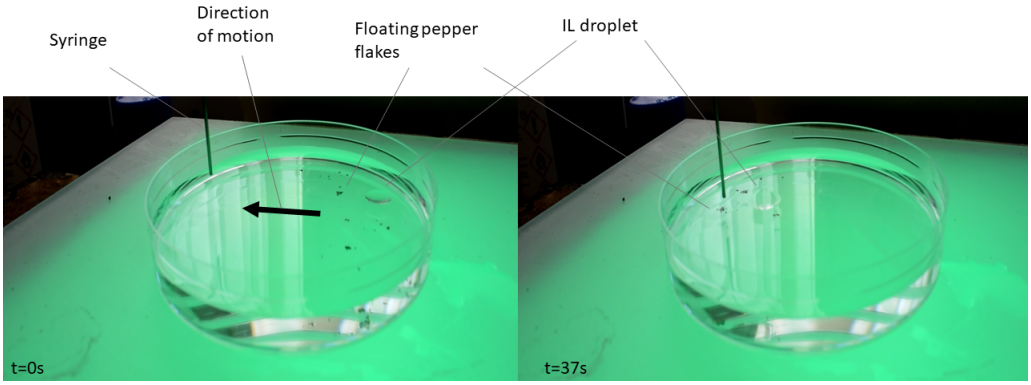

Figure 2.2: t = 0 s: A drop of IL is added to a solution of 0.1 M HCl and pepper flakes are sprinkled randomly on the surface. t = 37 s: A drop of chloroform is suspended above the surface (approx. 2 cm) which makes the pepper flakes assemble below the droplet.

2.2 Analytical Techniques

2.2.1 MatLab Code

Merging Experiments

The quantification of the merging system was achieved using code that was developed by Katherine Carter on Matlab. For the merging experiments (Figure 2.1(b)), the videos taken were analysed to obtain the velocities of the droplets. This code finds the centre of the droplet and records its position and radius in each frame (Figure 2.3(b)). Since the time between frames is already known due to the cameras frame rate, velocity data is extracted when the individual frames analysed are iterated over the entire video. The displacement of the droplets is obtained in pixels but converted into centimeters using the size of the plastic petri dish in the frames (9 cm diameter). The force on the droplets were calculated using the Steady-State Navier-Stokes equation,

$$F_v = 3\pi R\eta_s v_{ss}, \tag{2.2.1}$$

Where F_v is the force on the droplet at steady state, R is the radius of the droplet, η_s is the viscosity of the solution and v_{ss} is the velocity of the droplet at steady-state. The assumptions made in order to use this equation are that viscous drag forces on the droplets are equal to the net force on the droplets when they are moving at steady state, only half of the droplet is submerged, and the droplets are treated as solid spheres in the mathematical derivation. The equation is derived form the equation for viscous drag force,

$$F_{visc} = 2\pi R\eta_s V\frac{2+3\mu}{1+\mu}, \tag{2.2.2}$$

Where F_{visc} is the viscous drag force, V is the velocity of the droplet and μ is the ratio $\frac{\eta_d}{\eta_s}$ where η_d is the viscosity inside the droplet. Since the droplets are assumed to be solid spheres, η_d becomes much bigger than η_s and so the equation becomes

$$F_v = 6\pi R\eta_s v_{ss}, \tag{2.2.3}$$

This equation is then divided by 2 to obtain the original Equation (2.3.1) since only half of the droplet is assumed to be submerged. Since a droplet is not actually a solid hemisphere, instead of being 3, the real-life integer coefficient of the Navier-Stokes equation is between 2 (empty bubble) and 16/3 (flat disk) so there is some error in the force calculations. Steady-state velocity refers to the state of the droplet where its velocity is

unchanging. Figure 2.3(a) shows a velocity vs time graph of an analysed droplet to give an example of what is considered ”steady-state” in graphical terms. It is important to note that the floating IL droplet is blown by mouth and stuck to the side of the petri dish to prevent the IL droplet merging with the self-assembling droplets. The self-assembling droplets are then dispensed on the opposite side of the petri dish. Each data point obtained using this method is an average of 10 repeats.[44]

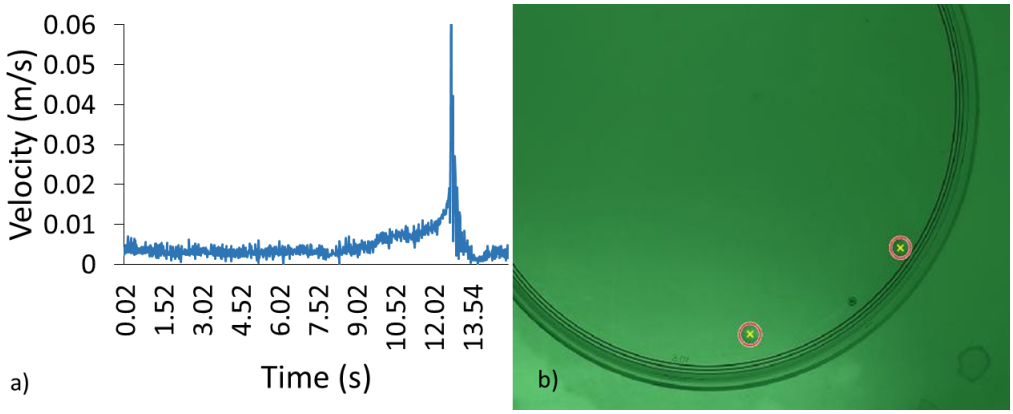

Figure 2.3: a) The velocity vs time graph of a droplet when moving towards another droplet. The peak at t = 12.6 s is due to sudden acceleration of the two droplets when merging. The average velocity between t = 2 s to t = 8 s would be considered as steady state. b) The detection of the droplets by the code.

Pepper Experiments

We found that any inert particle (such as a pepper particle) floating on the surface also directionally moves towards the self-assembling droplets. This phenomenon was quantified using another programme that was also developed by Katherine Carter on Matlab. The programme tracks the pepper particles as they move along the surface by binarising the image and finding the boundaries of each particle (Figure 2.4(a)). The velocity is calculated the same way as the merging code. When the videos are taken, the IL is dispensed onto the surface and the floating droplet is blown by mouth to the side of the petri dish in order to fix its position. Pepper is then sprinkled around the area where the IL droplet is and the self-assembling droplet is dispensed 7 cm away from the IL droplet. The pepper particles then move towards the self-assembling droplet (Figure 2.4(b)). Each data point obtained using this method is an average of 10 repeats.

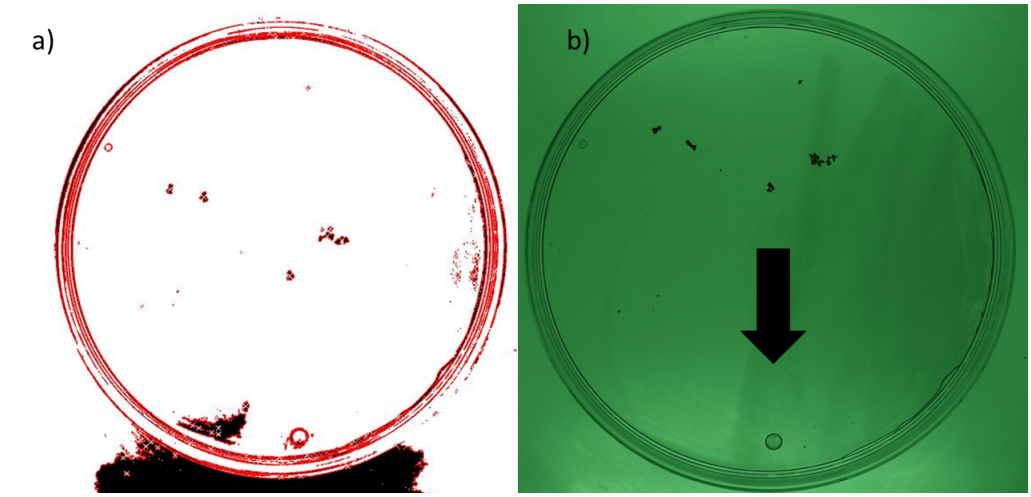

Figure 2.4: a) Image of how the code detects the pepper particles. b) A typical pepper experiment. Pepper particles floating on the surface move towards the self-assembling droplet.

2.2.2 Langmuir Trough

Surface tension values were obtained using the Wilhelmy plate method on the KSV NIMA Langmuir-Blodgett Trough (Model: AAC100419). The trough was filled with solution. A platinum plate 10 mm high and 20 mm wide was lowered into the solution. The force on the plate was measured to determine surface tension. The forces acting on the plate initially include its weight, force due to surface tension and its buoyancy,

$$F = mg + 2\gamma(t+w)\cos\theta - p_l g t w h, \tag{2.2.4}$$

where F is the force on the plate, γ surface tension, m, t and w are the plate mass, width and height, g is gravitational acceleration, $\theta is the contact angle, p_l the liquid density and h is the depth at which$ = 0 and h = 0 which reduces the equation to

$$F = mg + 2\gamma(t+w), \tag{2.2.5}$$

the force is then measured by the balance and since all other values are now known, surface tension can be calculated.[45] The plate used is made of platinum for increased wetting. Figure 2.3 shows the apparatus set-up.

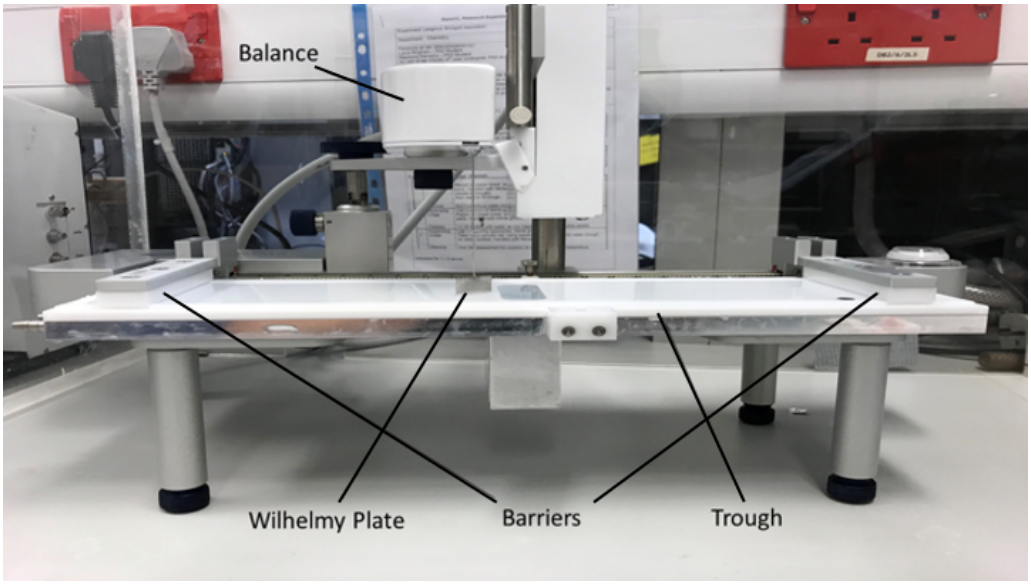

Figure 2.5: The Langmuir Trough used to take surface tension measurements.The platinum Wilhelmy plate is level with the surface of the water and is attached to the balance that measures the force on it. The barriers need to be at opposite end of the trough.

Advancing and Receding Contact Angle

Two distinct methods were used to take surface tension measurements of surfactants while using the Langmuir Trough. Method 1 consisted of dipping the Wilhelmy plate in the substrate (usually water) to note down its surface tension and then adding a drop of surfactant onto the substrate while the Wilhelmy plate is still in contact with it. Method 2 consisted of taking the Wilhelmy plate out of the substrate before adding the surfactant and then dipping it back into the substrate that is now covered with a monolayer of surfactant. The two methods yielded different results for certain surfactants.

Table 2.1: Surface tension values obtained for 0.5 M Octylamine in IL using the two methods.

Surfactant	**Substrate**	**γ of Substrate (m/Nm)**	**γ of Surfactant**	
			Method 1	**Method 2**
0.5M Octylamine in IL	Water	72.09	31.40	29.89

This could be happening due to the formation of a hydrophobic film on the Wilhelmy plate. The formation of this film would cause a variation in the contact angle and prevent it from being exactly zero. The difference between the two methods is how the

non-zero contact angle is formed. Method 1 would form a receding contact angle since the Wilhelmy plate is already in contact with the substrate, and Method 2 would form an advancing contact angle since the Wilhelmy plate is introduced to the substrate after the formation of the monolayer. Which means $\theta_1 < \theta_2$ and hence $cos\theta_1 > cos\theta_2$. According to Equation 2.2.4, this would mean that a higher surface tension value would be generated using Method 1. All surface tension measurements presented in this document are measured using Method 1.

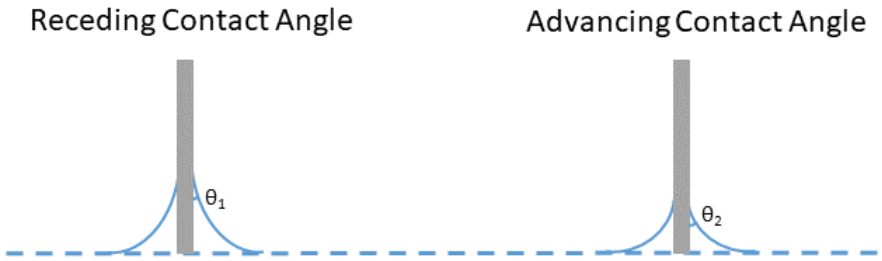

Figure 2.6: The difference between an advancing and receding contact angle on a Wilhelmy plate (grey).

Cleaning Procedure

Obtaining accurate surface tension measurements requires diligent cleaning of all glassware and equipment involved. The cleaning procedure followed before taking surface tension measurements involved brushing the trough and barriers with the detergent Decon-90®, rinsing once with UHQ water, rinsing with ethanol and rinsing 30 more times with UHQ water.The glassware in which the solution to be tested is kept is also cleaned with Decon-90®, rinsed with acetone and rinsed with UHQ water. Once the solution is in the trough, the surface of the solution is cleaned with a vacuum to make sure there is nothing on the surface that might change the surface tension of the solution. The Wilhelmy plate is flame cleaned using a Bunsen burner to remove any organic impurities.

2.2.3 NMR Experiments

^{1}H Nuclear Magnetic Resonance (NMR) was used to measure the amount of IL in a self-assembling droplet at a given time point. A drop of IL was deposited on a petri dish full of 0.1 M NaOH and the position of the IL droplet was fixed by blowing on the water by mouth in order to get the floating IL droplet to stick to the side of the petri dish. A drop of the

self-assembling droplet in question was then added to the solution. After the set amount of time, the droplet was taken off the surface using a clean syringe and was dispensed into an NMR tube that contained a known quantity of an NMR standard. The standard used was sodium trimethylsilylpropanesulfonate (DSS) and the NMR solvent used was DMSO-d^6. Each data point obtained from these experiments is an average of 5 repeats.

2.2.4 Hansen Solubility Parameters

Calculating Hansen solubility parameters is a way of predicting whether one material will dissolve in another. These were calculated using HSPiP®software. It operates on the basis that alike materials will dissolve in each other. Each molecule is given three Hansen parameters:

- δ_d The energy from dispersion forces
- δ_p The energy from dipolar intermolecular forces
- δ_h The energy from hydrogen bonds.

These are treated as coordinates in the Hansen space. The closer two substances are to each other in the Hansen space, the more likely they are to dissolve in each other. The software computes this information about a given substance by gathering information about what that substance is soluble in. For example, if a substance dissolves in substance A and B, the coordinates of that substance in Hansen space will be halfway between A and B. The value gets more precise as more information is gathered about the substance. Once an accurate value is obtained, a value called the interaction radius (R_0) is given to the substance in question. This is the distance between the substance in question and the substance that it is least soluble in (but still soluble in) in Hansen space. The distance between two Hansen parameters is calculated using the following equation:

$$(\mathrm{Ra})^2 = 4(\delta_{d2} - \delta_{d1})^2 + (\delta_{p2} - \delta_{p1})^2 + (\delta_{h2} - \delta_{h1})^2, \tag{2.2.6}$$

where Ra is the distance between two Hansen parameters and $\delta_{d1}, \delta_{p1}, \delta_{h1}$ and $\delta_{d2}, \delta_{p2}, \delta_{h2}$ are the Hansen solubility parameters of substances 1 and 2.[46] Dividing this number by the interaction radius gives the relative energy difference of the system (RED):

$$\mathrm{RED} = \mathrm{Ra}/\mathrm{R}_0, \tag{2.2.7}$$

the smaller the RED of a substance, the better it will dissolve in the material in question.

2.3 Materials

All chemicals used were purchased from Sigma Aldrich®or Fisher®. Toluene was passed through a glass pipette filled with Aluminium Oxide for purification.

2.4 Ion-exchange of the IL

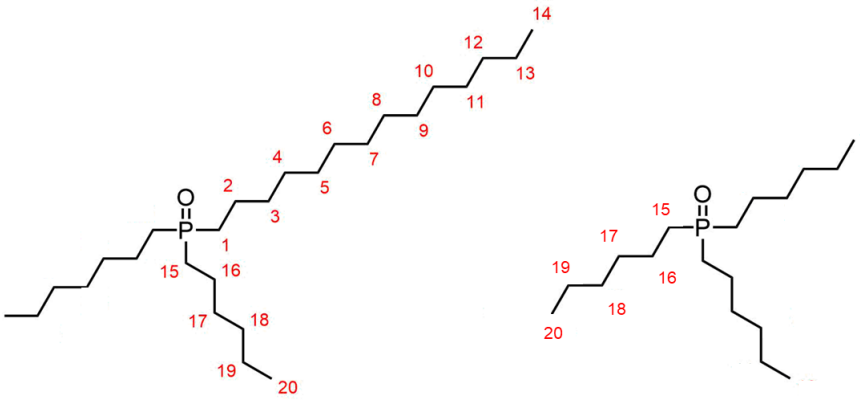

The conversion of trihexyltetradecylphosphonium chloride to trihexyltetradecylphosphonium hydroxide was attempted using an ion exchange resin (Amberlyst®A26 hydroxide form). The resin was placed in a column (60mm diameter, 6 inch depth) and washed once with methanol (300 ml). Thetrihexyltetradecylphosphonium chloride (4.02g) was dissolved in methanol (3ml) and the mixture applied to the column. The column was then washed with methanol (300ml) and the fraction collected. The methanol was removed *in vacuo* and the resulting oil washed with toluene (3x20ml). The oil was then dried under high vacuum yielding a red solid (4.09g). According to analytical data, what was actually made was a mixture of dihexyltetradecylphosphine oxide and trihexylphosphine oxide.[47] These are products of the decomposition of trihexyltetradecylphosphonium hydroxide.

NMR spectra were recorded on either a Bruker Avance III (400 MHz for ^{1}H; 101 MHz for ^{13}C) or a Varian VNMRS-600 (600 MHz for ^{1}H; 151 MHz for ^{13}C) and were processed using *MestreNova* (V 12.0.4). The NMR solvent used was $CDCl_3$. ^{1}H NMR (599 MHz, Chloroform-d) δ 1.68 – 1.61 (m, 8H, H1 and H15), 1.54 (dqd, J = 15.7, 7.8, 7.3, 3.8 Hz, 8H, H3 and H17), 1.41 – 1.36 (m, 8H, H2 and H16), 1.32 – 1.23 (m, 32H, H4-13 and H18 and H19), 0.91 – 0.84 (m, 12H,H20 and H14).13C NMR (151 MHz, $CDCl_3$) δ 31.89 (C19), 31.31 (C18), 30.91 (d, $^{3}J_{CP}$=8Hz, C2), 30.81 (d, $^{3}J_{CP}$= 8 Hz, C16), 29.65 (C11), 29.63 (C10), 29.62 (C9), 29.60 (C8), 29.56 (C7), 29.37 (C6), 29.32 (C5), 29.11

(C4), 28.18(d, $^3J_{CP}$= 37Hz, C15), 27.75 (d, $^3J_{CP}$= 37 Hz, C1) , 22.66 (C12), 22.41 (C13), 21.68(d, $^3J_{CP}$= 4Hz, C3), 21.65 (d, $^3J_{CP}$= 4 Hz, C17), 14.08 (C14), 13.98 (C20). TOF-MS (ASAP+): 303.58 (M+, 19%), 303.27 (69%), 304.28 (29.5%), 415.40 (31%), 605.55 (39%), 717.68 (57%), 718.69 (29%).

The relevant viscosity measurements were taken by Katherine Carter. They were taken at 25°C using an AR200 (TA Instruments) with a double concentric cylinder (DCC) attachment, which is surrounded by a heat bath to ensure isothermal temperature control, and a HR2-discovery rheometer (TA Instruments),with a peltier plate to control the temperature using a 60 mm, 4° cone.

Chapter 3

Results and Discussion

This section is split into three parts. In the first part, data collected on the possible factors that might be part of or indicate the underlying mechanism such as the surface tension of the substrate when its constituents are changed and the change in the rate of droplet motion with the change in the physical properties of the self-assembling droplet are presented. Considering this data, the feasibility of possible mechanisms of motion are then explored. In the second part, factors affecting the rate of droplet motion are presented and the reasons for them explained. Lastly, observed phenomena that could not be sufficiently explained through the course of this research project are presented and some possible explanations are given.

3.1 The Underlying Mechanism

3.1.1 Langmuir Trough Results

Table 3.1: Surface tension of the ionic liquid (IL) trihexyltetradecylphosphonium chloride measured on different aqueous substrates including the standard errors obtained from 5 experiments. This table shows that there is no statistically significant change in surface tension on different substrates.

Surfactant	Substrate	γ of Substrate (mN/m)	γ of Surfactant (mN/m)
IL	Water	72.1 ± 0.4	33.40 ± 0.4
IL	0.1M HCl	71.85 ± 0.4	32.58 ± 0.4
IL	0.1M NaOH	72.30 ± 0.4	32.12 ± 0.4

The surface tension of the IL on different aqueous substrates was measured using the Langmuir Trough. This was done in order to check if there was any significant change in the surface activity of the IL on different substrates. Although there is some variation, the change in surface tension is statistically insignificant for the purposes of this study.

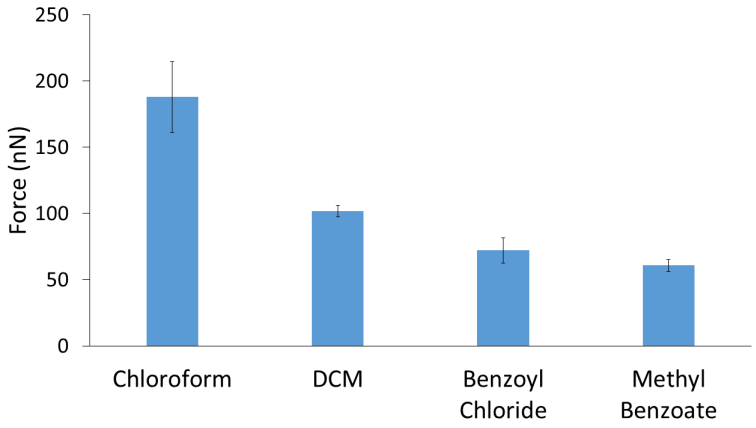

Figure 3.1: The variation in force acting upon a droplet that is moving towards the other (identical) droplet when the constituent of the droplet is changed with the floating IL adhered to the edge of the petri dish. The droplets in question purely contain chloroform, dichloromethane (DCM), benzoyl chloride or methyl benzoate. Substrate used is an aqueous solution of 0.1 M HCl. The error bars represent the standard error value obtained from 10 experiments. The figure shows that changing the solvent inside the self-assembling droplets changes the rate of merging.

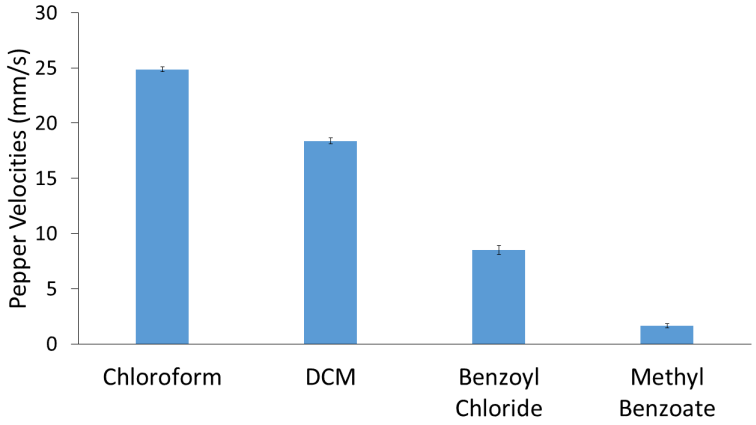

Figure 3.2: The variation in the velocity of the pepper particles floating on the aqueous substrate towards one droplet (as opposed to two in Figure 3.1) when the constituent of the droplet is changed. The droplet in question purely contains chloroform, DCM, benzoyl chloride or methyl benzoate. Substrate used is an aqueous solution of 0.1 M HCl. The error bars represent the standard error value obtained from 10 experiments. The figure shows that changing the solvent inside the self-assembling droplet changes the velocity of pepper movement.

3.1.2 Change in the Rate of Droplet Motion with Varying Droplet Constituents

The velocities of the self-assembling droplets when moving towards each other were measured and the forces acting on them calculated. Figure 3.1 shows that changing the solvent inside the self-assembling droplets changes the rate of merging. The velocities of peppers when moving towards a single self-assembling droplet was measured. Figure 3.2 shows that changing the solvent inside the self-assembling droplet changes the velocity of pepper movement. The fact that a similar trend is seen in the merging experiments (chloroform highest, methyl benzoate lowest) is seen in the pepper experiments, could mean that one of the dominate forces causing droplet self-assembly is flows on the surface of the substrate. In other words, one droplet is largely responsible for the rate of motion of another. The reason for this trend in the speed of motion is currently unclear. From Table 3.2, it can be seen that the only physical property that correlates with the rate of motion is density. This could be due to the fact that heavier droplets deform the surface more. However, experiments described below show that the ”Cheerios Effect” cannot explain the experimental observations. It is currently unclear why there is a correlation and unknown if it is even significant.

Table 3.2: Physical properties of the droplets that might affect droplet motion on the liquid surface. Surface tension (γ) values reported at 293.15 K (see Ref[48]) vapour pressure (P) values at 293.15 K (see Ref[49]), viscosity values (η) at 298.15 K (see Ref[50]) and density (ρ) values at 298.15 K (see Ref[51]). The perimeter of hexane was too faint to be detected by the MatLab code so its radius (r) could not be measured and the value reported is qualitative. The values reported for force on the droplets when merging (F) and pepper velocity (v) for toluene and mesitylene are also qualitative for the same reason. The toluene and mesitylene droplets were clear enough for the radius to be measured in one frame but not clear enough for it to be measured accurately in each frame. All radius values were taken for a 7 μl droplet on 0.1 M HCl. The standard error values were each obtained from 10 experiments.

Droplet	γ **(mN/m)**	r **(mm)**	η **(mPa s)**	P_v **(mmHg)**	ρ **(g/ml)**	F **(nN)**	v **(mm/s)**
Chloroform	27.20	3.23 ±0.14	0.566	153.0	1.48	188 ±27	24.9 ±0.6
DCM	27.84	3.08 ±0.13	0.406	353.4	1.32	102 ±4	18.4 ±0.8
Benzoyl Chloride	39.17	3.50 ±0.01	1.244	0.387	1.21	72 ±10	8.5 ±1.3
Methyl Benzoate	39.03	3.21 ±0.06	1.851	0.275	1.09	61 ±5	1.7 ±0.6
Toluene	28.53	4.33 ±0.14	0.554	22.47	0.87	<61	<1.7
Mesitylene	28.00	5.20 ±0.21	0.661	1.843	0.86	<<61	<<1.7
Hexane	18.46	>0.520	0.310	118.0	0.66	0	0

3.1.3 Possible Mechanisms for Motion

Temperature-Induced Motion

This mechanism is based on the latent heat of evaporation of the droplets. The self-assembling droplets evaporate and cool the surface surrounding them. The decrease in temperature causes an increase in the surface tension. This results in an area of particularly low temperature and hence high surface tension between the two droplets. The droplets move up the surface tension gradient and coalesce (Figure 3.3).

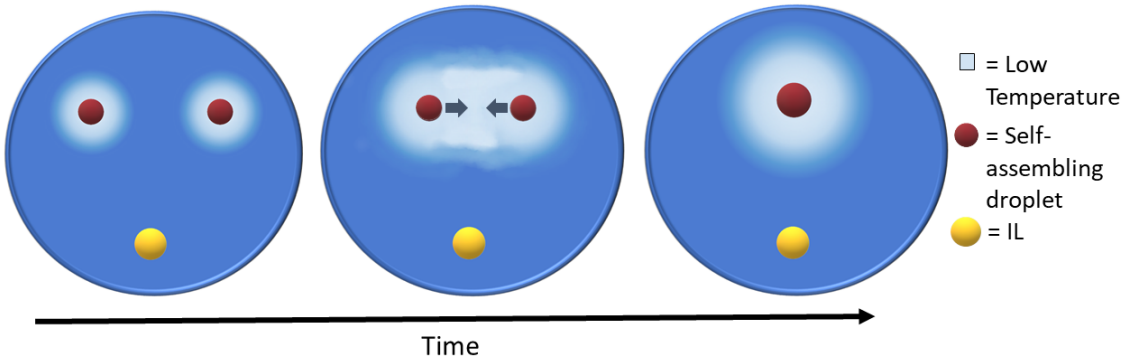

Figure 3.3: The two droplets cool the liquid surface surrounding them, creating an area of low temperature and hence high surface tension. The droplets move towards the area of high surface tension via Marangoni flows.

This mechanism is likely to be part of what is going on since many droplets used are volatile at room temperature (Table 3.2). This effect has also been reported by Liu *et al* when they used droplets made of 50% IPA in aqueous solution on an oil surface.[16]The latent heat of evaporation caused the droplets to assemble.

Evidence Against

This mechanism was tested by placing a chunk of ice in the corner of the petri dish full of aqueous solution. The pepper particles on the surface of the solution did not move towards the chunk of ice. This experiment was repeated by suspending a pellet of dry ice over the surface of the solution. There was again no movement of the pepper particles towards the area of low temperature. If thermal Marangoni effects were the dominant mechanisms for motion, one would also expect that the rate of motion would be determined by the volatility of the droplets. Referring to Table 3.2, it can be seen that there is no trend of increasing rate with increasing vapour pressure (and hence volatility).

This mechanism also does not explain the need for the presence of the IL droplet.

The Cheerios Effect

This mechanism is best explained using Sylgard®184 elastomer base as the self-assembling droplet. This is because it can form a droplet on the surface of an aqueous substrate without the presence of an IL monolayer. Other droplets simply spread across the surface due to the high surface tension of water but the same argument is valid for them as well. When two droplets of Sylgard®184 are deposited on the aqueous surface, they are motionless. The addition of the IL to the surface causes a decrease in the surface tension of the aqueous substrate, making the droplets curl up. The decrease in surface tension means that the intermolecular forces on the surface of the substrate are weaker and the two droplets now bend the surface more than they did before the IL was added. The two droplets then move towards each other like two basketballs on the skin of a trampoline (Figure 3.4).

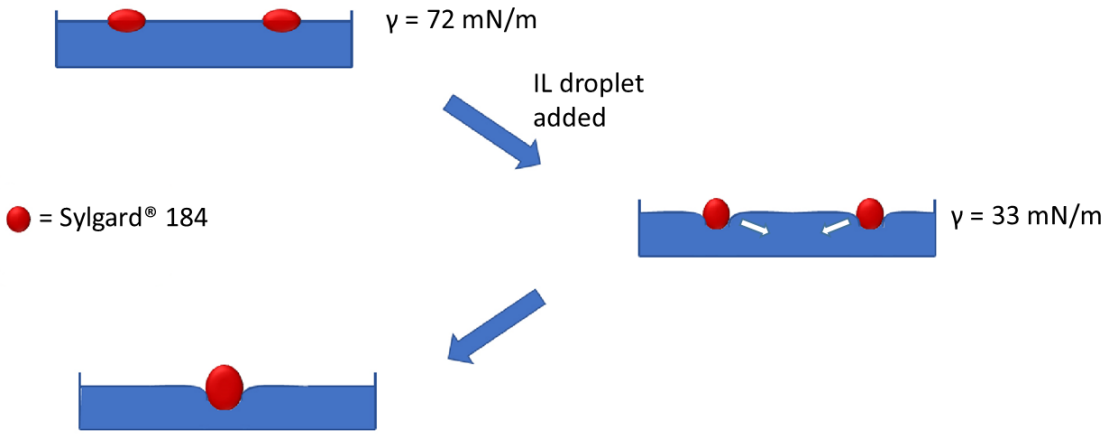

Figure 3.4: Two droplets of Sylgard®184 showing self-assembling behaviour due to the Cheerios Effect. The addition of IL onto the surface reduces the surface tension of water and causes the two Sylgard®184 droplets to bend the surface more than they did before the IL was added. The two droplets then move towards each other like two basketballs on the skin of a trampoline.

Evidence For

This is an effect that is present in a variety of droplet self-assembly systems and it makes sense that it should be a contributing factor to the rate of motion in this one. Referring to

Table 3.2, the increase in the force on the droplets when merging with increasing density is supports this notion. Heavier droplets would bend the surface more and hence move towards each other faster.

Evidence Against

This mechanism does not explain the movement of floating particles (such as pepper) towards benzoyl chloride. In order for two particles to exhibit the Cheerios Effect, they have to bend the surface in the same way. Pepper particles do not bend the surface so the reason they move towards the droplets in the presence of a monolayer of IL cannot be due to the Cheerios Effect. Also, according to this hypothesis, the IL can be replaced by any surfactant that will lower the surface tension of water low enough. This was tested experimentally using soap and it is not the case. In addition to this, for droplets less dense than water, there is no meniscus formed around the droplet that can be seen with the naked eye. This indicates that the Cheerios Effect is not long-ranged enough to be the dominant mechanism for motion.

The Dissolution of IL via Chemical Potential Gradient

This mechanism involves the uptake of IL from the monolayer into the self-assembling droplet along a chemical potential gradient. The droplet initially contains less IL than the surface so, according to Equation 1.4.6, has a lower chemical potential. According to Equation 1.4.5, a decrease in chemical potential is accompanied by a decrease in Gibbs free energy. Therefore, it is thermodynamically favourable for IL to move from the surface into the droplet. This results in the generation of areas of low IL concentration and hence high surface tension around the self-assembling droplets. The region between the droplets is depleted by both droplets so surface tension between the droplet becomes higher than the opposite sides of the droplets. The droplets move towards this region via surface Marangoni flows and coalesce (Figure 3.5).

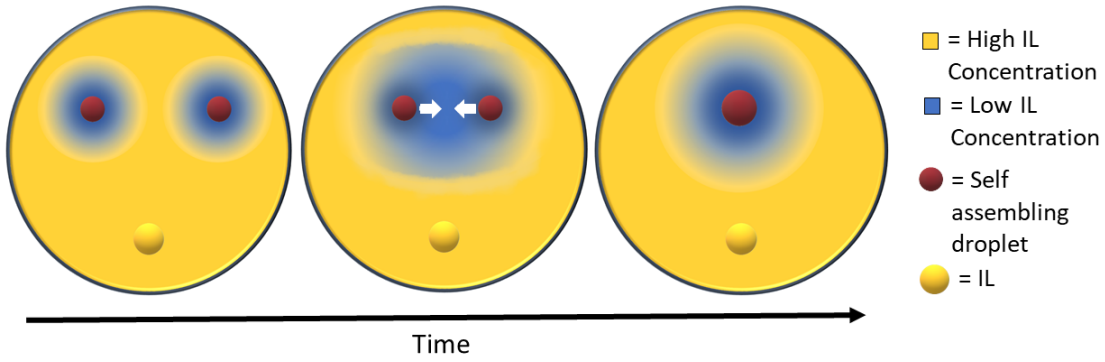

Figure 3.5: The IL on the surface moves into the two self-assembling droplets, creating an area of low IL concentration and high surface tension. The two droplets move towards this area and coalesce.

Evidence For

This mechanism was tested by measuring the amount of IL in a droplet that is on an aqueous surface covered in a monolayer of IL at given time points using ^{1}H NMR. The droplets chosen were a droplet purely composed of mesitylene and a droplet purely composed of benzoyl chloride because pure mesitylene droplets do not show directional motion on an aqueous substrate composed of 0.1 M NaOH, whereas benzoyl chloride droplets do. The amount of IL in both droplets were measured at t = 2 min and t = 10 min. According to

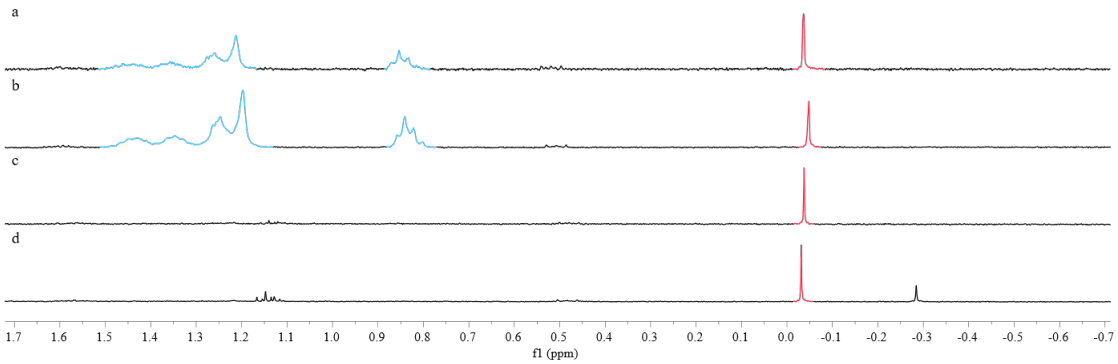

Figure 3.6: ^{1}H NMR spectrum of the droplets syringed off the surface of the aqueous solution of 0.1M NaOH covered in IL. The droplets were left on the surface for either 2 or 10 minutes. The standard peak is shown in red and the IL peaks are shown in light blue. a) Benzoyl chloride after 2 minutes. b) Benzoyl chloride after 10 minutes. c) Mesitylene after 2 minutes. d) Mesitylene after 10 minutes.

Table 3.3 and Figure 3.6, for droplets composed of benzoyl chloride, there is an increase

Table 3.3: The amount of accumulated IL in a drop of benzoyl chloride and a drop of mesitylene after being left on the surface of a 0.1 M aqueous solution of NaOH covered in IL surfactant for 2 and 10 minutes with standard errors obtained from 5 repeats. Table shows that a self-assembling droplet (benzoyl chloride) shows an uptake and increase in the amount of IL over time and a droplet that is not self-assembling (mesitylene) does not.

Droplet	Time (min)	Mass of IL(μg)
Benzoyl Chloride	2	7.7 ± 1.2
Benzoyl Chloride	10	17.5 ± 2.9
Mesitylene	2	0
Mesitylene	10	0

in the amount of IL inside the droplet over time. For droplets composed of mesitylene, there is no uptake of IL within 10 minutes that is detectable by ^{1}H NMR. It can be inferred from this that droplets that cause directional motion show an uptake of IL and droplets that do not cause directional motion do not uptake IL at all.

Another experiment was done by dyeing the IL droplet in Rhodamine B. The dyed IL was deposited onto a petri dish filled with an aqueous solution of 0.1 M NaOH and the petri dish was placed under a UV light source. Subsequently, a drop of benzoyl chloride was deposited onto the surface. After a few minutes, it was observed that the benzoyl chloride droplet turned fluorescent pink (Figure 3.7). This was also done with multiple droplets of benzoyl chloride on the surface to give the same results.This shows that substances can travel from the IL droplet, along the surface, into the self-assembling droplets.

The Hansen solubility parameters of different solvents regarding the IL were calculated using HSPiP software. From Table 3.4, it can be seen that the ranking order for the solubility of the IL in different solvents is not exactly replicated in the rates of droplet motion of droplets of those solvents shown in Table 3.2. Although, it is important to note that the method used to calculate the Hansen solubility parameters of the IL is not as reliable for ionic liquids as it is for organic liquids. Despite this, broadly, the RED is least for the chlorinated methanes, which show the greatest speeds, and largest for hydrocarbons that show the lowest speeds, with polar aromatics in-between. This is consistent with a solubility argument.

Figure 3.7: Figure showing the transfer of material from the IL droplet over the surface of water towards the benzoyl chloride droplet. t = 20 s : The dyed IL droplet is deposited onto the surface. t = 35 s: The benzoyl chloride droplet is deposited onto the surface. It is initially undyed. t = 500 s: The benzoyl chloride droplet is dyed fluorescent pink. This is evidence that material is transferred from the IL droplet, into the self-assembling droplet.

Table 3.4: The relative energy difference (RED) of various solvents when compared to the IL. These values were obtained by taking into account the solubility of the IL in 28 different solvents. The ones presented here are deemed the most relevant. The lowest RED values indicate the highest solubility of IL in that solvent. Generally it can be said from the table that IL is most soluble in chlorinated methanes, least soluble for hydrocarbons, with polar aromatics in-between.

Solvent	RED
DCM	0.388
Chloroform	0.620
Methyl Benzoate	0.700
Benzoyl Chloride	0.750
Toluene	0.892
Hexane	0.999
Hexadecane	1.000
Mesitylene	1.000
Water	2.312

If enough IL is added to the self-assembling droplet such that the chemical potential of the surface and the droplet are equal, the droplet stops moving. This is consistent with the origin of motion being a chemical potential gradient. The concentration of IL needed for this varies with the droplet constituent due to the varying degrees of solubility of the IL in the solvent. It should be also be noted that the IL is soluble in all droplets used in this project.

Evidence Against

Figure 3.8 shows the change in the force on the self-assembling droplets as they are moving towards each other with increasing concentration of IL inside the droplet. If the force on the droplets was determined by a chemical potential gradient, one would expect a logarithmic decrease in the force on the droplets with increasing concentration since the chemical potential of the droplet would increase logarithmically according to Equation 1.4.6. However, Figure 3.8 shows a decrease and then an increase in the force on the droplets after 0.04 M. This means that there are forces other than those caused by a chemical potential gradient affecting the rate motion of the droplet.

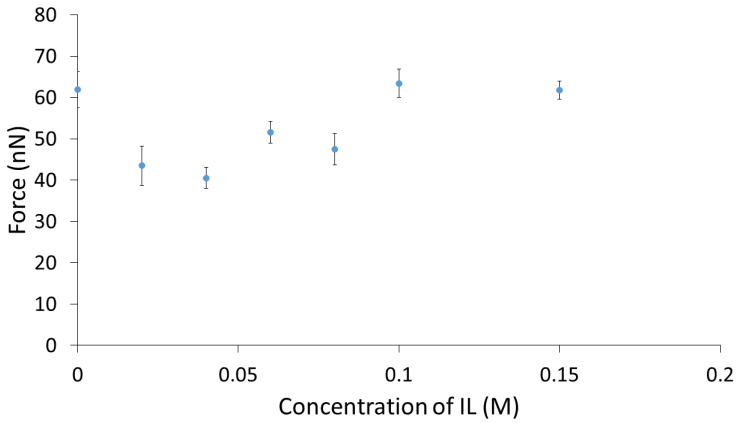

Figure 3.8: Plot showing the change in the force on the merging droplets with increasing concentration of IL inside the droplet. Substrate used is an aqueous solution of 0.1 M HCl. The IL droplet initiating motion is stuck to the side of the petri dish and the merging droplets are on the opposite side of the petri dish. The error bars represent the standard error values, each obtained from 10 experiments. Figure shows that the force on the droplets increases after 0.04M which would not happen if the rate was purely controlled by a chemical potential gradient.

Makowska *et al.*[52] reported that the solubility of the IL in alkanes decreases as the

chain length increases. If solubility was rate determining, a droplet consisting of hexane would move faster than droplets containing hexadecane. On the contrary, hexane droplets do not show any motion in any aqueous substrate where hexadecane droplets do. Although it should be noted here that hexane drops are very thin and the rate of transport into the droplet is proportional to the thickness of the droplet as well as the chemical potential gradient (see section on factors affecting the rate of motion of droplets). Plus the hexane evaporates quickly from the edge which would increase the local IL concentration. These could be one of the contributing factors to why hexane does not show motion.

3.1.4 Summary

The hypotheses Temperature-Induced Motion and the Cheerios Effect have been rejected as the primary cause of motion in this self-assembly system. It was found that they are not long ranged or comprehensive enough to fully explain the observations. The transfer of surfactant molecules from the surface into the droplet along a chemical potential gradient seems to be the most likely explanation for the motion but it cannot fully explain the trends in the rate of motion.This will be explored in the following section.

3.2 Factors Affecting Rate of Droplet Motion

3.2.1 Lensing

Lensing is a phenomenon that refers to the morphology of a droplet on the surface. The higher the contact angle, the more lensed the droplet is. The contact angle depends on the surface tension of the droplet (Figure 1.5). In the case of droplets containing IL, the contact angle depends both on the concentration of IL in the droplet and the distribution of IL in the droplet. Two droplets of the same constituents and the same concentration of IL can have different water-droplet-air contact angles and hence varying degrees of lensing (Figure 3.9). An unlensed droplet in this case refers to a droplet having the smallest observed contact angle at that concentration of IL and a lensed droplet refers to a droplet having the highest observed contact angle for that concentration of IL. It is important to note here that the amount of lensing is a continuous spectrum and whether a droplet is lensed or unlensed is determined subjectively by observations made by myself. The difference in contact angle is most likely due to the amount of time the droplet to be dispensed spends on the tip of the needle of the syringe. The solvent that the IL is

dissolved in evaporates faster than the IL and evaporates fastest at the surface of the droplet. Therefore, the longer the amount of time the droplet spends on the tip of the needle, the higher the concentration of IL at the surface of the droplet and therefore the lower the surface tension. The lower the surface tension of the droplet, the smaller the contact angle (Figure 1.5).

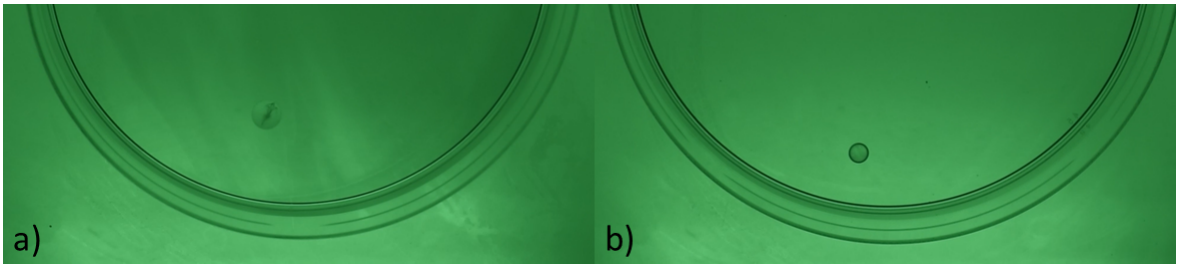

Figure 3.9: Two droplets of 0.15 M IL in benzoyl chloride on 0.1 M HCl with varying amounts of lensing. a) unlensed. b) lensed. Lensed droplets have a higher contact angle than unlensed ones.

Rate of Pepper Motion

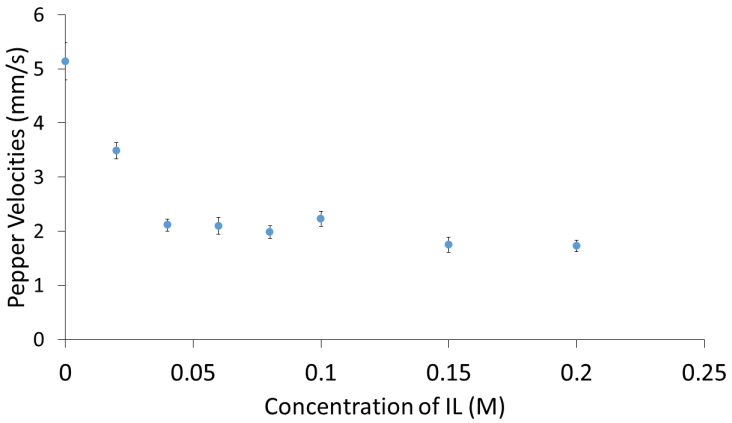

Figure 3.10: The velocity of the pepper particles moving towards the unlensed benzoyl chloride droplet at differing IL concentrations. The IL droplet is stuck to the edge of the petri dish and the pepper particles are placed around the stuck droplet. The pepper particles then move towards the self-assembling droplet. Substrate is an aqueous solution of 0.1 M HCl. The error bars represent the standard error values each obtained from 10 experiments. The figure shows an overall decrease in pepper velocity with increasing concentration of IL inside the self-assembling droplet.

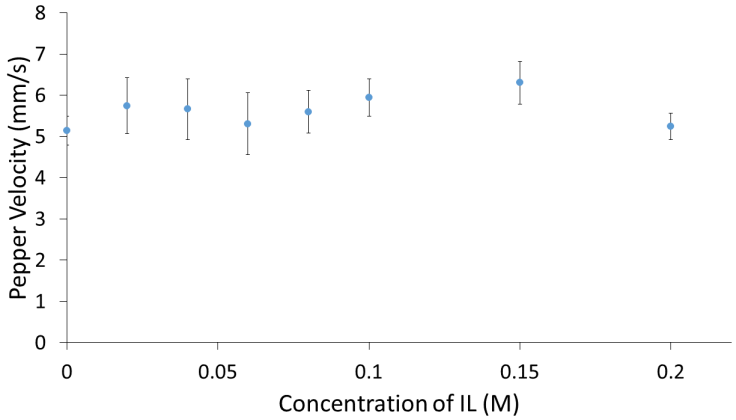

Figure 3.11: The velocity of the pepper particles moving towards the lensed benzoyl chloride droplet at differing IL concentrations. The IL droplet is stuck to the edge of the petri dish and the pepper particles are placed around the stuck droplet. The pepper particles then move towards the self-assembling droplet. Substrate used is an aqueous solution of 0.1 M HCl. The error bars represent the standard error values each obtained from 10 experiments. The figure shows no statistically significant change in pepper velocity with increasing IL concentration inside the self-assembling droplet.

Figure 3.10 shows a decrease in the velocity of pepper motion with the concentration of IL inside the benzoyl chloride droplet when the droplet is ”unlensed”. Figure 3.11 shows that when these droplets are lensed, the data are invariant within error so there is no statistically significant trend. This indicates the morphology of the droplet is a factor that affects the rate of pepper movement. It is important to note here that pepper velocity represents the rate of IL transfer into the droplet. The faster the peppers move, the faster IL is taken up off the surface by the droplet.

One explanation for why lensed droplets take up IL faster than unlensed ones is the differential speed of the convective flows within the droplets (Figure 3.12). The faster the convective flows, the more rapidly the IL molecule taken up by the droplets can be transferred to the bulk of the droplet and so the faster the concentration gradient between the edge of the droplet (the entry point of the IL) and the surface is replenished. The reason the convective flows within lensed droplets are faster can be understood from the following equation:

$$E = \eta(\frac{dv}{dn})^2, \tag{3.2.1}$$

where E is the energy dissipation per unit volume, η is the dynamic viscosity of the droplet and $\frac{dv}{dn}$ is the velocity gradient normal to the droplet interface.[53] For a constant amount

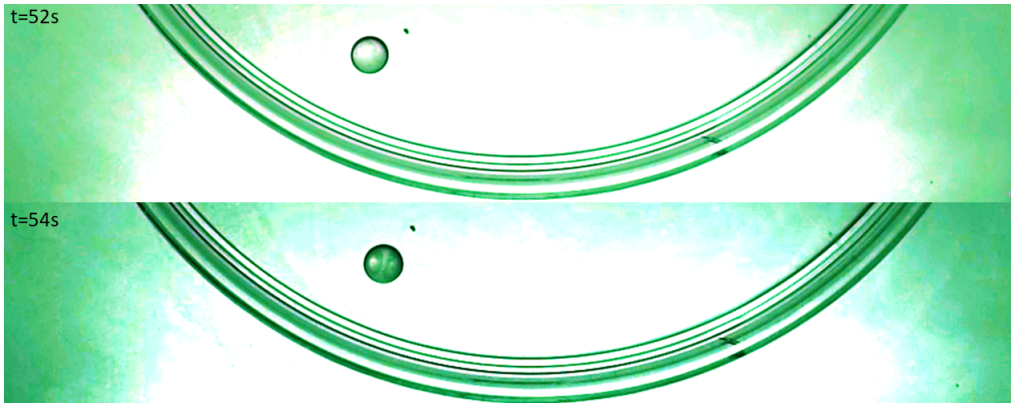

Figure 3.12: t = 52 s: Pure benzoyl chloride droplet when it is first introduced to the surface. Convective flows cannot be seen. t = 54 s: Enough hydrolysis has occured such that the movement of the hydrolysis products can be seen in the shape of convective flows.

of energy to be dissipated (amount of IL entering the droplet), the velocity gradient must also be constant. Therefore, if the contact angle and hence the height of the droplet decreases, the velocity of the convective flows will decrease to keep the velocity gradient constant. This effect is explained more clearly in Figure 3.13. The invariance of the rate of pepper motion with IL concentration for lensed droplets is caused by the circulation of IL within the droplet no longer being the rate determining step for pepper motion. The rate determining step becomes the rate of IL intake across the three point contact line which does not vary with the concentration of IL inside the droplet.

Figure 3.14 shows an increase in the unlensed benzoyl chloride droplet radius with increasing concentration of IL. The increase in radius is most likely due to the decrease in the contact angle of the benzoyl chloride droplet caused by the decrease in the surface tension of the droplet. So, an unlensed droplet containing 0.2 M IL in benzoyl chloride has a lower contact angle than that of a droplet containing 0.02 M IL in benzoyl chloride. The decrease in pepper velocity in unlensed droplets with increasing IL concentration in Figure 3.10 may then be associated with the decrease in lensing.

The logarithmic increase in droplet radius in Figure 3.14 indicates that there should be a logarithmic decrease in the pepper velocity in Figure 3.10 if the reason for the decrease is the size of the contact angle. The reason the pepper velocity levels out instead of a logarithmic decrease for concentrations above 0.04 M may be because of the increase in the perimeter of the droplets. As the contact angle decreases, the perimeter of the

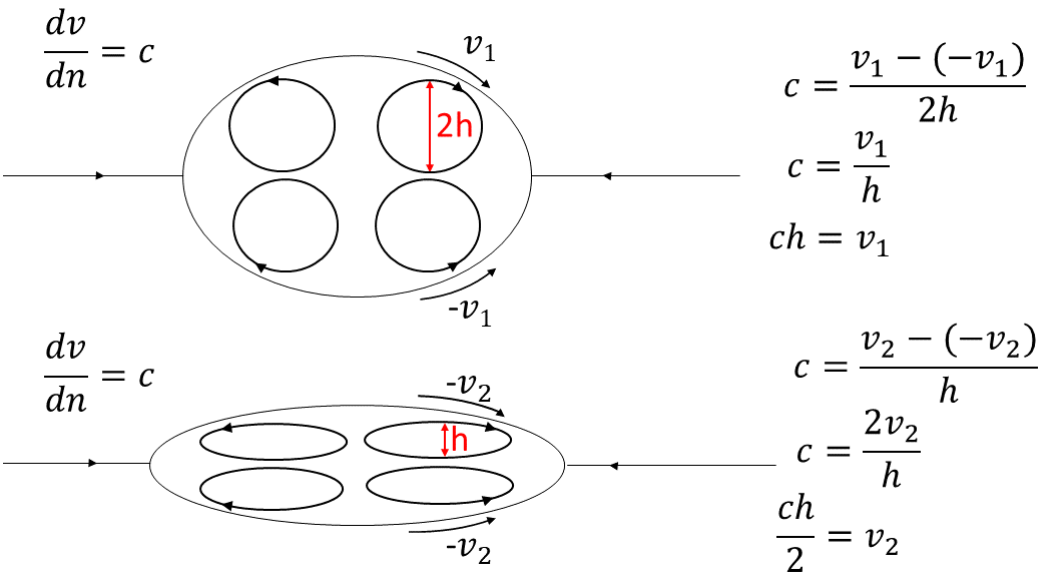

Figure 3.13: Two droplets on an aqueous surface containing the same concentration of IL but varying widths. The change in the velocity of convective flows with decreasing droplet height. The velocity of the convective flows decrease with decreasing droplet height due to the constant energy of dissipation.

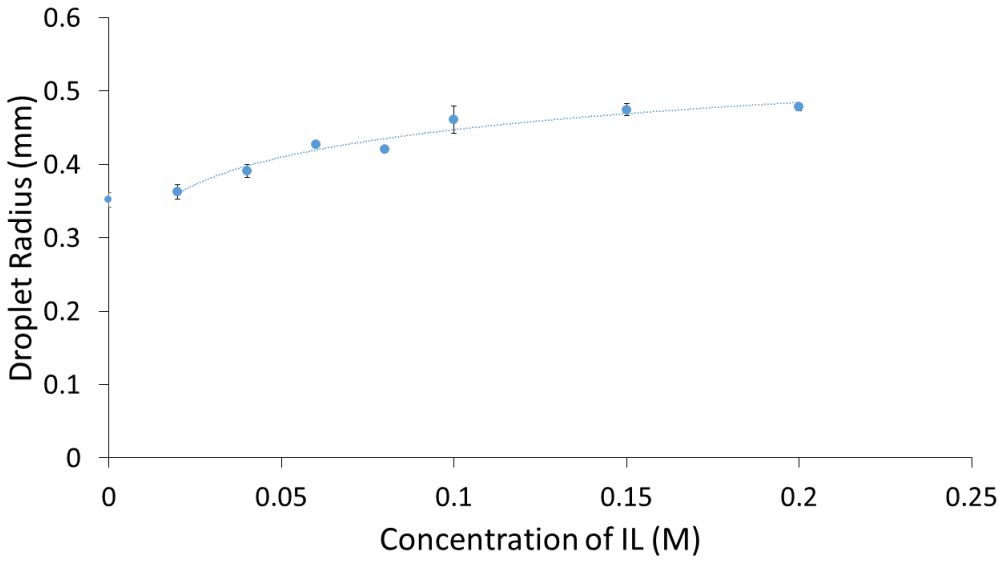

Figure 3.14: Plot of benzoyl chloride droplet radius taken from a bird's-eye view vs IL concentration inside the droplet. Logarithmic line of best fit included. R^2 = 0.95. Substrate used is an aqueous solution of 0.1 M HCl. The error bars represent the standard error values, each obtained from 10 experiments.

droplets on the surface becomes larger. Therefore, there are more available entry points through which IL from the surface can diffuse into the droplet. This causes an increase in the rate of uptake of IL and thus an increase in the pepper velocity for that concentration of IL. This effect causes the benzoyl chloride droplets with IL concentrations higher than 0.04 M to exhibit higher pepper velocities than if the velocities were purely determined by the contact angle. It should be noted that this explanation only makes sense if after 0.04 M, the length of the perimeter of the droplets increases faster than the speed of the convective flows decreases. This information could not be gathered during the course of this project due to time constraints.

3.2.2 Rate of Droplet Merging

The rate of droplet merging is different to the rate of pepper particle motion. Pepper motion is an indication of how much IL is taken up by a lone droplet per unit of time. Merging droplets are subject to a greater variety of effects. The forces reported in this thesis are the net forces on the droplets when all of these effects are considered.

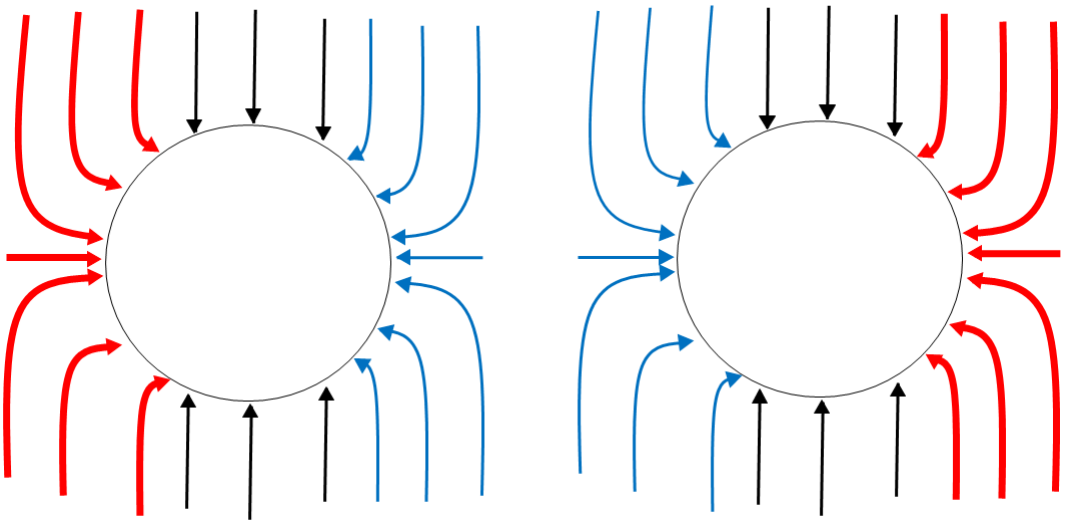

Figure 3.15: Figure showing the surface convective flows acting upon the droplets. Flows pushing the droplets together (red) are much stronger than the ones pushing them apart (blue).

Figure 3.15 shows the surface convective flows acting on two droplets on the same liquid surface. In order for the droplets to merge, the red forces need to be stronger than the blue. The blue and black forces are mainly caused by the IL uptake on the sides of the droplet that is not the anterior side.

Figure 3.8 shows the net force on a benzoyl chloride droplet when moving towards another identical benzoyl chloride droplet as the concentration of IL in the droplet increases. There is a decrease in the force on the droplets as concentration of IL increases for concentrations below 0.04 M. An explanation for this is that as the concentration of IL decreases, the lensing of the droplets increases so the droplet becomes better at taking up IL from the surface. This causes a larger IL concentration gradient between the surface of the substrate on the posterior and the anterior side of the droplets. This phenomenon is based on the fact that the substrate surface area on the anterior side of the droplets is always smaller than or equal to the area on the posterior side of the droplets. This is explained more clearly in Figure 3.16.

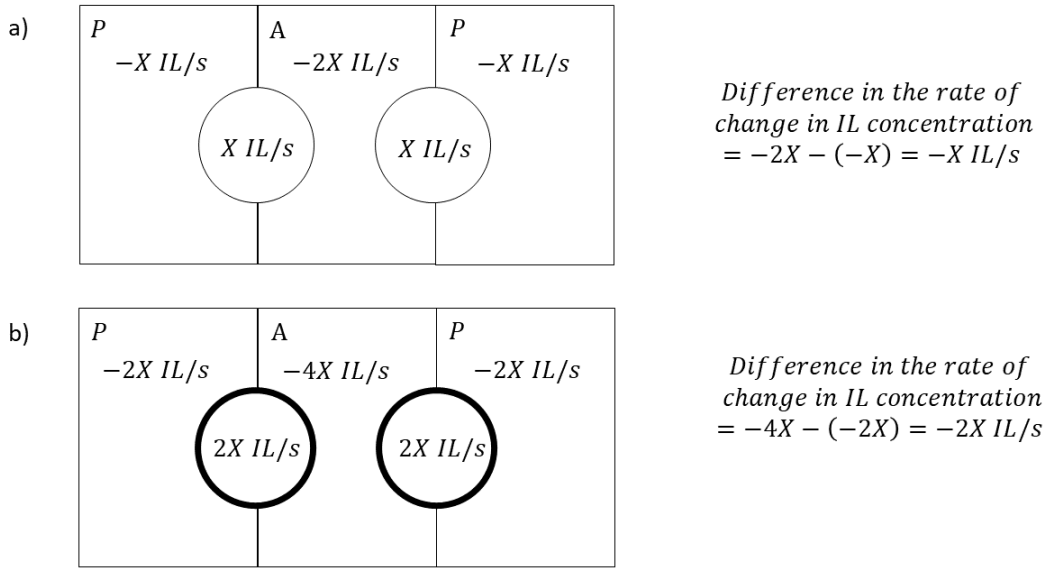

Figure 3.16: Difference in the rate of change of IL concentration between the posterior (P) and the anterior (A) sides of the droplets where the droplet is a) worse at taking in IL and b) better at taking in IL. X represents the amount of IL gained in an area per second. A larger concentration gradient formed for the droplets that are better at taking in IL.

The difference between the rate of uptake of IL from the posterior and the anterior side increases as the droplet gets better at taking in IL. If the surface area of the posterior side of a droplet is equal or greater than the anterior side, this causes the formation of a steeper surfactant concentration gradient and hence stronger convective flows towards the anterior. For concentrations above 0.04 M, lensing is no longer the driving force. As the concentration of IL increases, the perimeter of the droplets and hence the area of

contact of the droplet with the surface increases. This permits the droplet to take up more IL off the surface at one time. Using the same logic as lensing, this causes a steeper concentration gradient between the posterior and the anterior as the radius of the droplet increases and the droplets speed up. The force then levels out after 0.1 M as the droplet radius also levels out (Figure 3.14).

Bulk Fluid Motions

Merging can also be aided by bulk fluid motions. Surface flows that push the droplet against the surfactant concentration gradient are then diverted into the bulk. This then causes the formation of convective flows in the bulk. The water flows along the oil-water interface and the friction between the water and oil exert a force on the oil droplets that push the droplets even more against the surface tension gradient. These bulk flows are also formed by the flows on the anterior side of the droplets that oppose the overall motion but the convective flows on the anterior side of the droplets are smaller than that on the posterior side of the droplets due to the volume of liquid on the posterior being larger than the anterior (Figure 3.17).

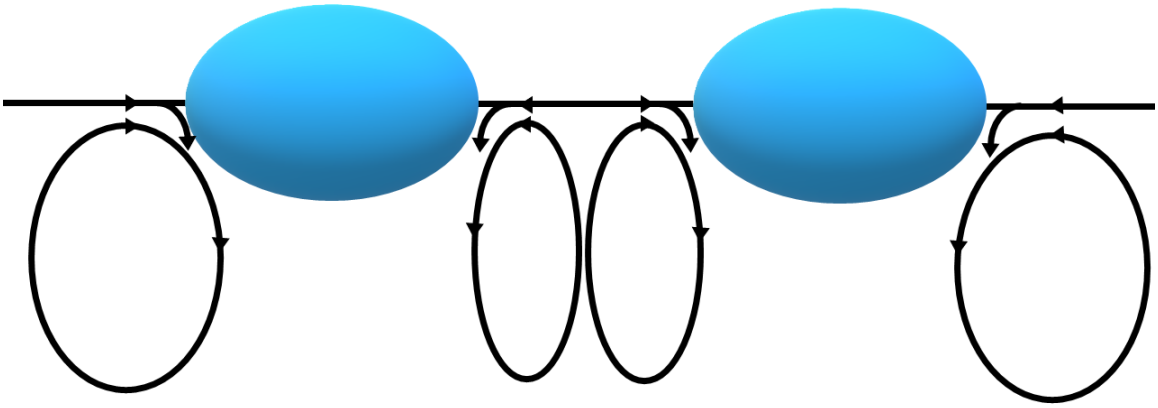

Figure 3.17: The bulk fluid motions acting upon two self-assembling droplets that increase the rate of droplet self-assembly. The bulk fluid motions on the posterior side of the droplets are stronger than the shared side of the droplets so they are pushed together.

This may be another reason why the force towards the area in between the droplets scales faster than the force towards the outside. As the droplets become better at taking up IL off the surface, the surface flows are faster and hence the bulk flows are faster.

3.3 Unexplained Phenomena

Throughout the course of this study, there were observed and quantified phenomena potentially important to the origin of the droplet motion that could not be fully explained. In this section I will present these observations and, for some of them, offer a possible explanation based on the evidence collected.

3.3.1 Droplet Motion on Different Aqueous Substrates

Origin of Droplet Motion on Different Aqueous Substrates

Table 3.5: The direction of motion of particles floating on the substrate covered in a monolayer of IL when the constituents of the substrate are changed. '+' represents particles moving towards the droplet, '-' represents particles not moving towards the droplet. The concentrations of all the aqueous substrates are 0.1 M.

Droplet	Water	HCl	NaOH	H_2SO_4	NaCl	Na_2SO_4
Chloroform	+	+	+	+	+	+
Dichloromethane	+	+	+	+	+	+
Benzoyl Chloride	+	+	+	+	+	+
Methyl Benzoate	+	+	+	+	+	+
Toluene	+	+	-	+	+	+
Mesitylene	-	+	-	-	+	-
Hexane	-	-	-	-	-	-
Hexadecane	+	+	+	-	+	+
2M Malononitrile in IL	-	-	+	-	-	+

The impact of a given droplet on the aqueous surface varies as the constituents of the bulk is changed. Table 3.5 shows that when the ions in the substrate are changed, certain droplets do not perturb the surface at all. An explanation for this is the counter-ion ion exchange of the IL in the monolayer. If the motion is on a substrate containing an anion other than Cl^-, the Cl^- counter-ion of the phosphonium would be exchanged for whatever that anion may be. This new phosphonium-anion complex cannot diffuse into the self-assembling droplet so there is no gradient in the IL concentration in the monolayer and so there is no surface tension gradient to cause droplet motion (Figure 3.18).

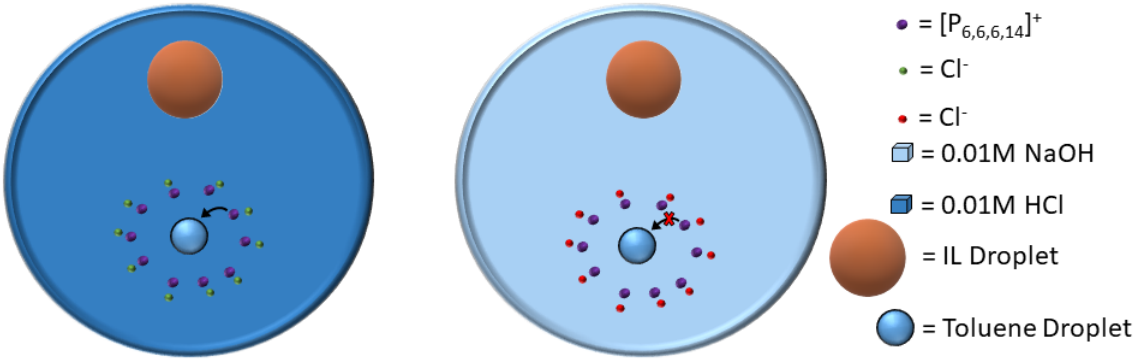

Figure 3.18: IL can be taken up by the toluene droplet on 0.1 M HCl since there is no ion exchange. IL cannot be taken up by the toluene droplet from the monolayer in 0.1 M NaOH due to the hydroxide-chloride ion exchange. If there is no IL taken up by the droplet, there is no surface tension gradient formed so no motion.

In an unpublished study, Francis *et al.* purchased the same phosphonium cation with a range of counter-ions other than Cl^- and observed that droplet motion showed a strong dependence on the nature of the counter-ion. To test this hypothesis, the replacement of the chloride ion of the IL with a hydroxide ion was attempted using an ion exchange resin. Mass spectrometry and NMR data indicate that what was made was a mixture dihexyltetradecylphosphine oxide and trihexylphosphine oxide which are products of the decomposition of trihexyltetradecylphosphonium hydroxide. Regardless of the identity, the product was tested. It was deposited on a pure water substrate and two droplets that do not exhibit motion on 0.1M NaOH but do exhibit motion on water (toluene) were added to the surface. The droplets showed motion. However, no conclusions can be made on the monolayer ion-exchange hypothesis.

Rate of Droplet Motion on Different Aqueous Substrates

It was observed that pepper particles floating on the surface are continuously repelled away from the floating IL droplet even in the absence of a self-assembling droplet. When an IL droplet is deposited on the surface, after the initial spreading, it exhibits a replenishing of the surfactant monolayer. Figure 3.19 shows the differing rates of replenishment via the velocity of pepper motion on different aqueous substrates. The reason for this could be due to the varying solubility of the IL in different ionic solutions.

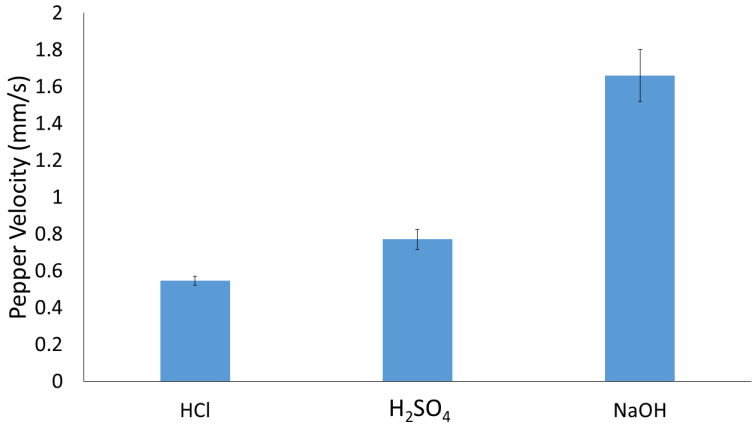

Figure 3.19: The variation in the rate of spreading of the ionic liquid monolayer replenishment with change in aqueous substrate. This was measured by using the velocity with which pepper particles were repelled when placed around the IL droplet that was stuck on the side of the petri dish. The error bars represent the standard error values, each obtained from 10 experiments.

Figure 3.20 shows that the change in the constituents of the aqueous substrate also affects the rate of merging of methyl benzoate. The reason the force on the methyl benzoate droplets is highest on 0.1 M HCl could be because of the higher solubility of the IL in 0.1 M NaOH. The more soluble the IL is, the less IL there is on the surface at any one time and hence less IL to be taken up by the methyl benzoate droplet, creating a smaller surface tension gradient.

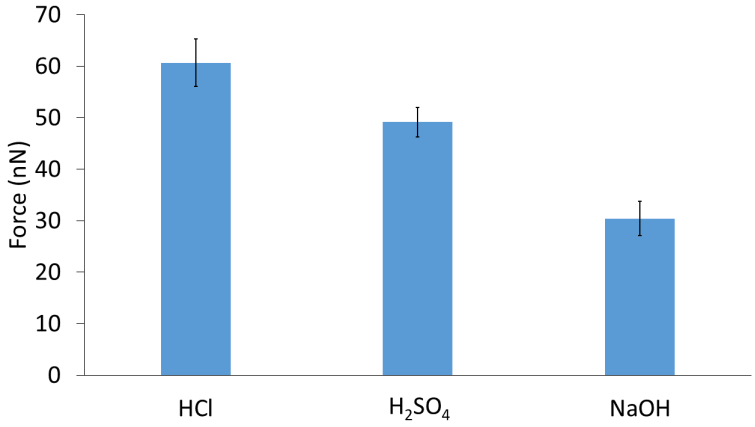

Figure 3.20: The variation in the force on a methyl benzoate droplet when moving towards another methyl benzoate droplet when the constituents of the aqueous substrate is changed. The IL droplet was stuck to the side of the petri dish and the self-assembling (methyl benzoate) droplets were placed on the opposite side of the petri dish. The error bars represent the standard error values, each obtained from 10 experiments.

3.3.2 Suspended Droplets

When a droplet of benzoyl chloride, DCM or chloroform at the tip of a needle is suspended above an aqueous solution of 0.1 M HCl covered with a monolayer of IL, pepper and droplets on the surface congregate under the suspended droplet. Whether the motion was temperature-induced was tested by suspending a piece of dry ice over the surface of the solution. No movement was observed so this hypothesis was rejected. The movement of the pepper might be due to the suspended droplet evaporating off the tip of the needle and condensing onto the water surface. The IL in that area dissolve into the condensed benzoyl chloride, DCM or chloroform which creates a surface tension gradient towards that area (Figure 3.21). The fact that the ranking of the velocity of pepper motion is qualitatively the same as if the droplet was on the surface (Table 3.2) supports this narrative.

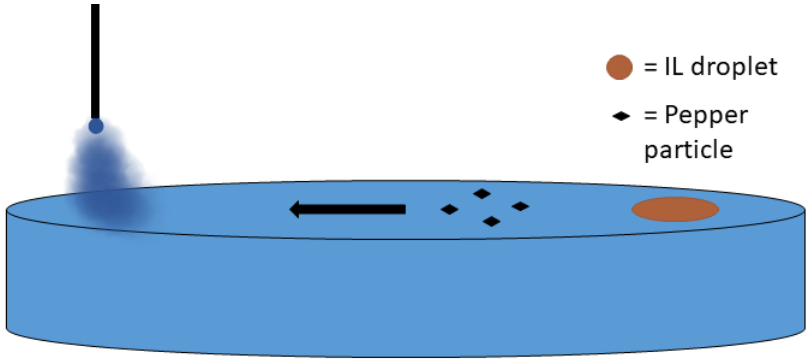

Figure 3.21: The suspended droplet evaporating and condensing onto the surface and creating a surface tension gradient which then causes the pepper particles to move towards that area.

3.3.3 Direction of Floating IL Motion

The direction of motion of the floating IL droplet depended on the constituents of the substrate. When on 0.1 M HCl, the IL droplet moved towards the self-assembling droplets. When on 0.1 M NaOH, the IL droplet moved away from the self-assembling droplets and towards the sides of the petri dish (Figure 3.22). The reason why the IL droplet would move towards the area of high surface tension on 0.1 M HCl but an area of low surface tension on 0.1 M NaOH remains unclear. It is also important to note that in the absence of the self-assembling droplets, the IL droplet still moved towards the side of the petri dish on 0.1 M NaOH where on 0.1 M HCl, the IL droplet remains stationary.

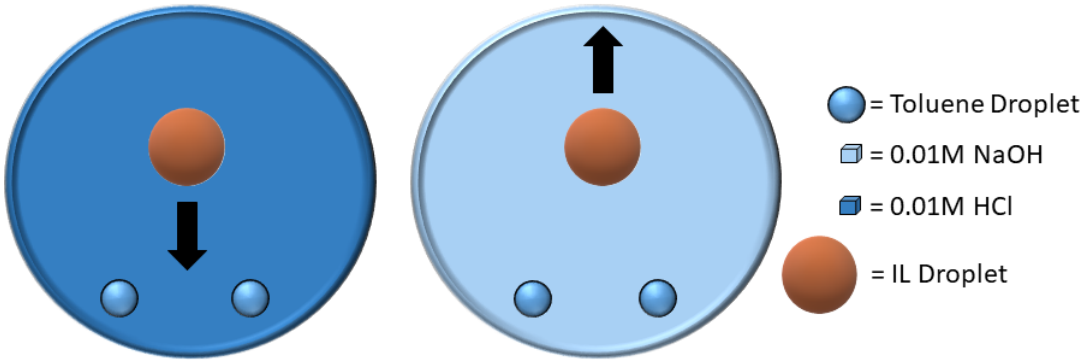

Figure 3.22: IL droplet moves towards the self-assembling droplets on 0.1 M HCl and away from them on 0.1 M NaOH.

3.3.4 Why this IL?

The reason why the motion of the self-assembling droplets towards each other only occurs with this IL and not with other surfactants is unclear. A property that the IL exclusively exhibits when compared to other surfactants tested (octylamine, soap and cetyltrimethylammonium bromide) is that the floating IL droplet seems to replenish the IL monolayer continuously (Figure 3.23). When the monolayer dissolves into the self-assembling droplet, the monolayer has to be replaced in order to maintain the surface tension gradient. This was tested using pepper particles. After any other surfactant was dispensed onto the surface, any pepper particle that was put on the surface remained stationary. With IL on the surface, a continuous repulsion of pepper particles could be observed for over 10 minutes. The property of the IL that causes this differential is unclear.

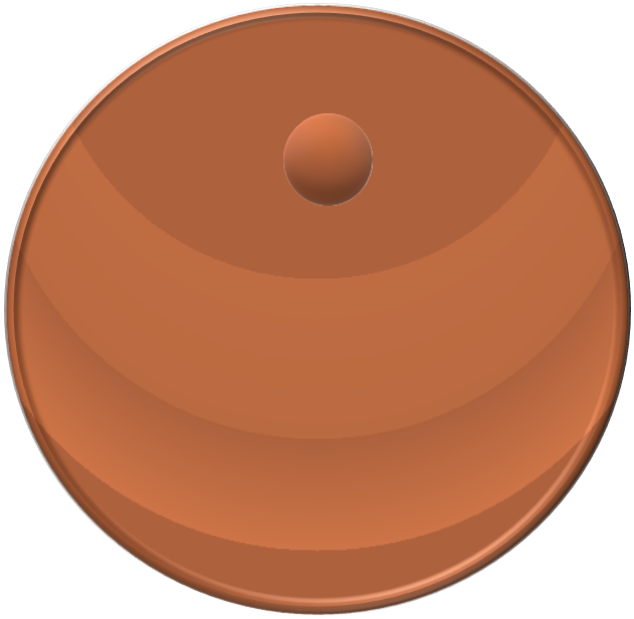

Figure 3.23: A figure depicting the hypothesised reason behind the motion being specific to this IL. When the IL droplet is on the surface, the monolayer of IL is continuously being replenished when it dissolves. This maintains the surface tension gradient and hence the droplet motion.

3.3.5 Droplet Prerequisites

The requirements for the solvent that makes up a droplet for it to exhibit self-assembling behaviour seem to be that the solvent should not be miscible in water and that IL should

be able to dissolve in it. All droplets that show motion fit this description. Even so, in order to support this claim one would need to find a solvent that isn't soluble in water and that the IL cannot dissolve in and show that it does not exhibit self-assembling behaviour. This solvent could not be found over the course of this project.

3.4 Other Experimental Results

There were many avenues explored in this project that lead to dead ends. Nevertheless, knowledge was gained from all of these avenues so even briefly, they need mentioning. At first, we thought the mechanism was extremely pH dependent because we thought that the hydrolysis of benzoyl chloride might play a role in it. A normal merging experiment was run with two droplets of 4 M benzoyl chloride in IL on aqueous solutions of 0.1 M HCl, 0.1 M NaOH, 0.1 M H_2SO_4, water, pH 4 0.1 M acetic acid buffer, pH 7 0.1 M phosphate buffer and pH 10 0.1 M carbonate buffer covered in a monolayer of IL. This was done in order to check the pH dependence of the mechanism because at first we thought that the hydrolysis of benzoyl chloride might play a role in the mechanism. Qualitatively, no noticeable changes in motion were observed.

The same merging experiment was done using saturated NaCl as the aqueous substrate. This was done in order to check if the system was influenced by a chloride gradient across the solution such as the one discussed by Francis *et al.*[37] The droplets were visibly slower, but they did coalesce. The slowness was most likely due to the increased viscosity of the solution.

Different concentrations (0-3 M) of glucose were added to the aqueous solution and the same merging experiment run. This was done in order to understand the effect of the change in the bouyancy of the solution to droplet motion. Although visibly slower, the droplets coalesced. Again, the slowness was most likely due to the increased viscosity of the solution.

Chapter 4

Conclusion and Further Study

4.1 Conclusion and Final Discussion

The motivation for this study was to determine the mechanism driving the motion of two droplets consisting of 4 M benzoyl chloride in trihexyltetradecylphosphonium chloride (IL) when a droplet consisting of 0.5 M octylamine in IL is added to the aqueous surface (0.1 M NaOH, 0.1 M HCl, 0.1 M H_2SO_4). The approach taken to achieve this was to simplify the system to two droplets consisting of one pure solvent (immiscible in water, soluble in IL) and a pure IL droplet. It was found that the effect also caused the motion of floating particles (pepper particles) on the surface and that the motion of both the particles and the droplets depended similarly on the identity of the solvent in the droplets.

The proposed origin of the motion was the dissolution of the IL monolayer into the self-assembling droplet. The reason for this dissolution is a difference in chemical potential between the droplet and the surface. The fact that the droplet contains a lower concentration of IL than the surface means that it has a lower chemical potential. The transfer of the IL from high to low chemical potential is thermodynamically favourable since it involves a decrease in Gibbs free energy (Equation 1.4.5 and 1.4.6). The existence of this chemical potential gradient was supported by the fact that the droplets stop working when the concentration of the IL inside the droplet is high enough for the chemical potential gradient to be in equilibrium. The proposed mechanism was supported by NMR studies that showed that the IL on the monolayer is transferred into a droplet that exhibits self-assembling behaviour and not transferred into droplet that does not (Figure 3.6). Temperature gradients and the Cheerios Effect were found insufficient to explain the full extent of motion.

However, it was found that the rate of droplet motion with increasing concentration of IL inside the self-assembling droplet was not determined by the steepness of a chemical potential gradient but the morphology of the droplet. The decrease in the rate of droplet motion with increased concentration of IL (Figure 3.8) was hypothesised to be due to the decrease in the size of the contact angle of the droplet with the surface and hence the height of the droplet. The thinner the droplet, the slower the internal convective

flows inside the droplet. According to the proposed mechanism, the IL that is taken in is transferred into the bulk of the droplets via convective flows so the faster the convective flows, the faster that IL will be transferred to the bulk so that more IL can be taken in. This helps generate a larger surface tension gradient and hence faster droplet motion. The increase in the rate of droplet motion after 0.04 M (Figure 3.8) was explained by the increase in the perimeter of the droplet. The bigger the perimeter, the more entry points there are for the IL molecules to transfer into the droplet. The force first decreases due to the shrinking of the contact angle and then increases due to the increase in the perimeter (Figure 3.14).

The effect of a change in the aqueous substrates on the rate of motion was studied. It was found that changing the constituents of the aqueous substrate not only changed the rate of droplet motion, but it also caused some droplets to stop moving entirely. The reason for this effect was found not to be due to an exchange of the counter-ion of the IL on the monolayer. The real reason for this is currently unknown. The reason for a change in the rate of motion with changing aqueous substrate is thought to be due to the varying solubility of the IL in different ionic solutions. The more soluble the IL in the substrate, the less it can dissolve in the self-assembling droplet so the smaller the surface tension gradient created will be.

In conclusion, an explanation for the underlying mechanism for the motion was determined. This system consistently exhibits droplet self-assembly and is the only droplet self-assembly system that can do this with this large of a variety of solvents with this many different means of controlling the rate. The droplets could be used as vessels for chemical reaction, vehicles for transport or even to replicate biological cells.

4.2 Further Study

There is a plethora of unknown phenomena that can be further studied in this system. As mentioned before, it is not known what governs the change in rate of motion for droplets of different solvents, why some droplets stop motion on different aqueous substrates or why they show different rates of motion on different substrates. But perhaps the most interesting question would be why this ionic liquid causes this sort of motion and whether it can be replicated using a different surfactant. It could also be useful to understand the effects of changing droplet size on the motion of the droplet. This was not studied due to time constraints.

4.2. Further Study

Another avenue of research could be to resume this study by taking some more analytical data. It would be interesting to be able to track convective flows using tracker particles in order to see flows on the surface and the bulk. This project was limited at times by the sensitivity of the MatLab code. If this could be improved or a better way of tracking the speed of droplets developed, a wider idea of the rate of droplet motion could be achieved.

Bibliography

[1] Fyen, W.; Holsteyns, F.; Bearda, T.; Arnauts, S.; Steenbergen, J. V.; Doumen, G.; Kenis, K.; Mertens, P. W. In *Developments in Surface Contamination and Cleaning (Second Edition)*; Kohli, R., Mittal, K., Eds.; William Andrew Publishing, 2008; Chapter 19, pp 800–802.

[2] Gugliotti, M.; Silverstein, T. *Journal of Chemical Education* **2004**, *81*, 67–68.

[3] Lautrup, B. In *Physics of continuous matter : exotic and everyday phenomena in the macroscopic world*; Spicer, T., Fielding, L., Laurenson, S., Eds.; IOP Publishing Ltd, 2005; Chapter 5, pp 97–106.

[4] Bonn, D.; Eggers, J.; Indekeu, J.; Meunier, J.; Rolley, E. *Reviews of Modern Physics* **2009**, *81*, 741–742.

[5] Wilkinson, K.; Bain, C.; Matsubara, H.; Aratono, M. *ChemPhysChem* **2005**, *6*, 547–555.

[6] Whitesides, G.; Grzybowski, B. *Science* **2002**, *295*, 2418–2421.

[7] Hatakeyama, T.; Chen, D.; Ismagilov, R. *J Am Chem Soc* **2006**, *128*, 2518–2519.

[8] Song, H.; Chen, D.; Ismagilov, R. *Angewandte Chemie* **2006**, *45*, 7336–7356.

[9] Teh, S.-Y.; Lin, R.; Hung, L.-H.; P.Lee, A. *Lab on a Chip* **2008**, *2*, 198–220.

[10] Chiu, D.; Lorenz, R.; Jeffries, G. *Analytical Chemistry* **2009**, *13*, 5111–5118.

[11] Chiu, D.; Lorenz, R. *American Chemical Society* **2009**, *42*, 649–658.

[12] Hatch, A.; Fisher, J.; Pentoney, S.; Yang, D.; Lee, A. *Lab on a Chip* **2011**, *15*, 2509–2517.

[13] Shestopalov, I.; Tice, J.; Ismagilov, R. *Lab on a Chip* **2004**, *4*, 316–321.

[14] Thutupalli, S.; Herminghaus, S.; Seemann, R. *Soft Matter* **2011**, *7*, 1312–1320.

[15] Parthiban, P.; Doyle, P.; Hashimoto, M. *Soft Matter* **2019**, *15*, 4244–4254.

[16] Liu, D.; Tran, T. *J. Phys. Chem. Lett* **2018**, *9*, 4771–4775.

[17] Lachr, S.; Yoon, S.; Grzybowski, B. *Chem. Soc. Rev.* **2016**, *45*, 4766–4796.

[18] Sourjik, V.; Wingreen, N. *Current Opinion in Cell Biology* **2011**, *24*, 262–268.

[19] Cortese, B.; Palama, I. E.; D'Amone, S.; Gigli, G. *Integrative Biology* **2014**, *6*, 817–830.

[20] Devreotes, P.; Janetopoulos, C. *Journal of Biological Chemistry* **2003**, *278*, 20445–20448.

[21] Paster, E.; Ryu, W. *PNAS* **2008**, *105*, 5373–5377.

[22] Yabunaka, S.; Ohta, T.; Yoshinaga, N. *The Journal of Chemical Physics* **2012**, *136*, 074904.

[23] Golestanian, R.; Liverpool, T.; Ajdari, A. *Phys. Rev. Lett.* **2005**, *94*, 220801.

[24] Herminghaus, S.; Maass, C.; Krüger, C.; Thutupalli, S.; Goehring, L.; Bahr, C. *Soft Matter* **2014**, *10*, 7008–7022.

[25] Yang, Z.; Wei, J.; Sobolev, Y.; Grzybowski, B. *Nature* **2018**, *553*, 313–318.

[26] Suetmatsu, N.; Saikusa, K.; Izumi, T. N. S. *Langmuir* **2019**, *35*, 11601–11607.

[27] Matsuno, H.; Hanczyc, M.; Ikegami, T. *Progress in Artificial Life* **2007**, *4828*, 179–188.

[28] Kruger, C.; Klos, G.; Bahr, C.; Maass, C. *Phys. Rev. Lett.* **2016**, *117*, 048003.

[29] Jin, C.; Hokmabad, B.; Baldwin, K.; Maass, C. *Journal of Physics: Condensed Matter* **2018**, *30*, 054003.

[30] Jin, C.; Kruger, C.; Maass, C. *PNAS* **2017**, *20*, 5089–5094.

[31] Schmitt, M.; Stark, H. *Physics of Fluids* **2016**, *28*, 012106.

[32] Atkins, P. In *Physical Chemistry Sixth Edition*; Tom Spicer, L. F., Laurenson, S., Eds.; Oxford University Press, 2000; Chapter 5.3, p 132.

[33] Ban, T.; Aoyama, A.; Matsumoto, T. *Chemistry Letters* **2010**, *39*, 1294–1296.

[34] Anderson, J.; Lowell, M.; Prieve, D. *Journal of Fluid Mechanics* **1982**, *117*, 107–121.

[35] Prieve, D.; Anderson, J.; Ebel, J.; Lowell, M. *Journal of Fluid Mechanics* **1984**, *148*, 247–269.

[36] Abécassis, B.; Cottin-Bizonne, C.; Ybert, C.; Ajdari, A.; Bocquet, L. *Nature Materials* **2008**, *7*, 785–789.

[37] Francis, W.; Fay, C.; Florea, L.; Diamond, D. *Chem. Commun.* **2015**, *51*, 2342–2344.

[38] Cira, N.; Benusiglio, A.; Prakash, M. *Nature* **2015**, *519*, 446–450.

[39] Ban, T.; Nakata, H. *The Journal of Physical Chemistry B* **2015**, *119*, 7100–7105.

[40] Francis, W.; Wagner, K.; Beirne, S.; Officer, D.; Wallace, G.; Florea, L.; Diamond, D. *Sensors and Actuators B: Chemical* **2017**, *239*, 1069–1075.

[41] Lagzi, I.; Soh, S.; Wesson, P.; Browne, K.; Grzybowski, B. *Journal of the American Chemical Society* **2010**, *132*, 1198–1199.

[42] Sellier, M.; Nock, V.; Verdier, C. *International Journal of Multiphase Flow* **2011**, *37*, 462–468.

[43] Vella, D.; Mahadevan, L. *American Journal of Physics* **2005**, *73*, 817.

[44] Herminghaus, S.; Maass, C.; Krüger, C.; Thutupalli, S.; Goehring, L.; Bahr, C. *Soft matter* **2014**, *10*, 7008.

[45] Wang, X.; Min, Q.; Zhang, Z.; Duan, Y.; Zhang, Y.; Zhai, J. *Colloids and Surfaces A: Physicochemical and Engineering Aspects* **2017**, *527*, 115 – 122.

[46] Hansen, C. *Hansen Solubility Parameters - A User's Handbook*; CRC Press, 2007.

[47] Pagilagan, R.; McEwen, W. *Chemical Communications* **1966**, *01002*, 652–653.

[48] Wohlfarth, C.; Wohlfarth, B. In *Landolt-Bornstein - Surface Tension of Pure Liquids and Binary Liquid Mixtures*; Lechner, M., Ed.; Springer, 1997.

[49] Yaws, C. L. *The Yaws Handbook of Vapor Pressure*; Elsevier, 2005.

[50] Wohlfarth, C. In *Landolt-Bornstein - Viscosity of Pure Organic Liquids and Binary Liquid Mixtures*; Martienssen, W., Ed.; Springer, 2008.

[51] Yaws, C. L. *Chemical Properties Handbook*; McGraw-Hill, 1999.

[52] Makowska, A.; Siporska, A.; Oracz, P.; Szydlowski, J. *J. Chem. Eng. Data* **2010**, *5*, 2829–2832.

[53] Holtzman, B.; Kohlstedt, D.; Morgan, J. *Journal of Petrology* **2005**, *46*, 2569–2592.